Electronic Supplementary Material (ESI) for Chemical Science.

Supporting Information

Photoswitchable dynasore analogs to control endocytosis with light

Núria Camarero[a,+], Ana Trapero[a,b,+], Ariadna Pérez-Jiménez[a], Eric Macia[c], Alexandre Gomila-Juaneda[a], Andrés Martín-Quirós[a,], Laura Nevola[d,j], Artur Llobet[e], Amadeu Llebaria[b], Jordi Hernando[f], Ernest Giralt[d,g] and Pau Gorostiza[a,h,i,*]

[a]Institute for Bioengineering of Catalonia (IBEC), The Barcelona Institute of Science and Technology (BIST); [b]Institute for Advanced Chemistry of Catalonia (IQAC-CSIC); [c]Institut de Pharmacologie Moléculaire et Cellulaire (IPMC) Université Nice Sophia Antipolis; [d]Institute for Research in Biomedicine (IRB Barcelona); [e]Bellvitge Biomedical Research Institute (IDIBELL); [f]Departament de Química, Universitat Autònoma de Barcelona (UAB); [g]Universitat de Barcelona (UB); [i]ICREA; [h]CIBER-BBN; [j]present address: IDP Discovery Pharma, Parc Científic de Barcelona (PCB)

Table of Contents

1. Synthesis

Dynazo-4 was prepared following the synthetic strategy described in Scheme 1 and experimental details are described below. Dynazo-2 and dynazo-3 were purchased from ASM Research Chemicals and their purity was assessed by HPLC, NMR and mass spectrometry analysis.

1.1 General methods

All moisture-sensitive reactions were carried out under nitrogen. All materials were obtained commercially and used without further purification. Solvents were dried prior to use with alumina in a solvent purification system or distilled and dried by standard methods. Reactions were monitored by thin layer chromatography (60 F, 0.2 mm, *Macherey-Nagel*) by visualization under a UV (254 nm) lamp. Flash column chromatography was performed using an Isolera Spektra One purification system and the appropriately sized Biotage SNAP column containing KP-silica gel (50 μm). The NMR spectroscopic experiments were carried out on a Variant Mercury 400 instrument (400 MHz for ^{1}H and 100 MHz for ^{13}C). Chemical shifts (δ) are given in parts per million (ppm) relative to the residual solvent peak (DMSO-d_6: ^{1}H, δ =2.50 ppm; ^{13}C, δ = 39.5 ppm), and the coupling constants (J) are reported in hertz (Hz). HRMS were recorded in a time-of-flight (TOF) mass spectrometer with electrospray ionization (ESI).

1.2. Experimental Procedures

(*E*)-4-((4-hydroxy-3-(methoxycarbonyl)phenyl)diazenyl)benzoic acid (5)

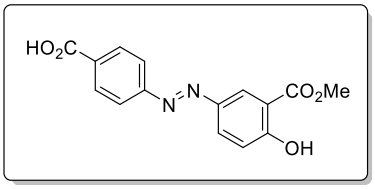

Concentrated HCl (3.0 ml, 37.2 mmol, 37% w/w) was added to a suspension of 4-aminobenzoic acid (3 g, 21.9 mmol) in H_2O (36 mL) at -5 ºC, and the resulting suspension was stirred at -5 ºC for 5 min.

To this solution, aqueous solution of $NaNO_2$ (1.6 g, 23 mmol) in H_2O (6 mL) was added at -5 ºC. The obtained diazotized solution was stirred at -5 to 0 ºC for 1 h. The resulting yellow suspension was slowly added to a precooled alkaline solution of methyl 2-hydroxybenzoate (3.4 ml, 26.3 mmol) in H_2O (63 mL) containing NaOH (1.7 g, 43.8 mmol) and Na_2CO_3 (4.6 g, 43.8 mmol) at 0 to -5 ºC. During the reaction the pH values was monitored and adjusted to a pH > 8 by adding additional 2M NaOH solution to the reaction mixture. After 3 h, the reaction mixture was cooled to -10 ºC and acidified to pH 2 with 6M HCl. The brown precipitate was filtered, washed with water and recrystallized from ethanol to afford compound **5** (4 g, 13.3 mmol, 61% yield) as a yellow solid. mp 301–302 ºC. ^{1}H NMR (400 MHz, DMSO-d_6) δ 8.33 (d, J = 2.6 Hz, 1H), 8.16–8.07 (m, 3H), 7.92 (d, J = 8.1 Hz, 2H), 7.20 (d, J = 8.9 Hz, 1H), 3.93 (s, 3H); ^{13}C NMR (100 MHz, DMSO-d_6) δ 167.9, 166.8, 162.8, 154.1, 144.4, 133.2, 130.5, 128.8, 126.2, 122.3, 118.9, 114.7, 52.6; HRMS calculated for $C_{15}H_{13}N_2O_5$: 301.0824 $[M+H]^+$. Found: 301.0873.

(*E*)-4-((3-(hydrazinecarbonyl)-4-hydroxyphenyl)diazenyl)benzoic acid (6)

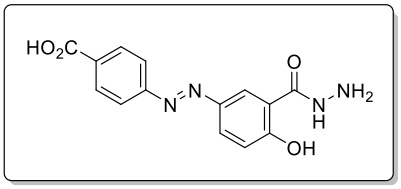

To a solution of **5** (4 g, 13.3 mmol) in EtOH (50 ml) was added $NH_2NH_2{\cdot}H_2O$ (4.1 ml, 53.3 mmol). The reaction mixture was stirred at reflux for 3 h. After cooling to RT, the solvent was removed to half of its original volume under reduced pressure. The resulting suspension was filtered, and the solid was washed with EtOH, and dried. The solid was suspended in H_2O and the suspension was cooled to 0 ºC and acidified to pH 2 with 1M HCl. The precipitate was filtered, washed with H_2O and EtOH, and dried to afford compound **6** (2.5 g, 8.3 mmol, 62% yield) as a brown solid. mp 166–168 ºC. ^{1}H NMR (400 MHz, DMSO-d_6) δ 8.30 (d, J = 2.8 Hz, 1H), 7.97 (d, J = 8.5 Hz, 2H), 7.66 (d, J = 8.2 Hz, 2H), 7.61 (dd, J = 9.2, 2.8 Hz, 1H), 6.36 (d, J = 9.2 Hz, 1H); ^{13}C NMR (100 MHz, DMSO-

d_6) δ 176.2, 169.0, 167.1, 154.6, 139.4, 138.5, 130.0, 129.7, 125.1, 123.0, 120.5, 118.0; HRMS calculated for $C_{14}H_{11}N_4O_4$: 299.0780 $[M–H]^-$. Found: 299.0781.

4-((*E*)-(3-((*E*)-2-(3,4-dihydroxybenzylidene)hydrazinecarbonyl)-4-hydroxyphenyl)diazenyl)benzoic acid (7)

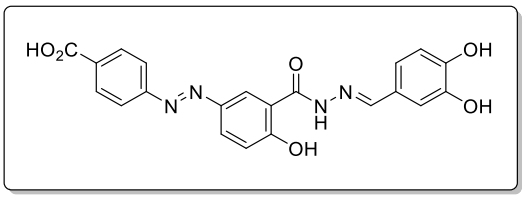

To a solution of **6** (0.36 g, 1.2 mmol) in EtOH (12 ml) was added TEA (0.17 mL, 1.2 mmol) and an equimolar amount of 3,4-dihydroxybenzaldehyde (0.17 g, 1.2 mmol) in EtOH (1 mL). The resulting suspension was heated to reflux for 18 h. The precipitate obtained was filtered off and washed with EtOH. The filtrate was purified by column chromatography (CH_2Cl_2/MeOH 15:1 with 0.06 to 0.2% AcOH) to afford compound **7** (0.42 g, 1.0 mmol, 83%) as an orange solid. mp 295–297 ºC. ^{1}H NMR (400 MHz, DMSO-d_6) δ 12.27 (bs, 1H), 9.44 (bs, 1H), 9.30 (bs, 1H), 8.56 (s, 1H), 8.29 (s, 1H), 8.13 (d, J = 8.4 Hz, 2H), 7.99 (dd, J = 8.9, 2.4 Hz, 1H), 7.92 (d, J = 8.4 Hz, 2H), 7.28 (d, J = 1.9 Hz, 1H), 7.03–7.11 (m, 1H), 6.98 (dd, J = 8.2, 1.5 Hz, 1H), 6.80 (d, J = 8.1 Hz, 1H); ^{13}C NMR (100 MHz, DMSO-d_6) δ 166.8, 163.8, 154.6, 149.4, 148.2, 145.7, 130.6, 126.6, 126.3, 125.5, 122.1, 120.9, 119.2, 116.8, 115.6, 112.8; HRMS calculated for $C_{21}H_{15}N_4O_6$: 419.0992 $[M–H]^-$. Found: 419.0995.

4-((*E*)-(3-((*E*)-2-(3,4-dihydroxybenzylidene)hydrazinecarbonyl)-4-hydroxyphenyl)diazenyl)-*N*-(2-morpholino-2-(pyridin-2-yl)ethyl)benzamide (Dynazo-4)

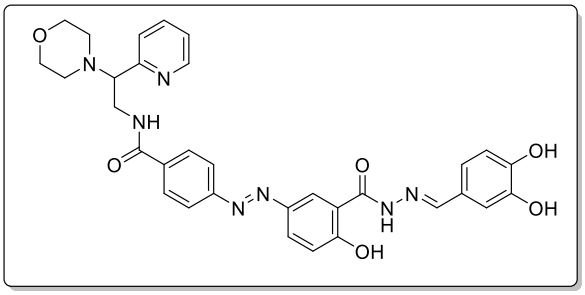

To a solution of **7** (0.06 g, 0.14 mmol) in DMF (4 ml), TEA (0.05 ml, 0.36 mmol), HOBt (0.03 g, 0.21 mmol) and EDC (0.04 g, 0.21 mmol) were added. The reaction mixture was stirred for 10 min followed by the addition of 2-morpholino-2-(pyridin-2-yl)ethanamine (0.036 g, 0.17 mmol). The mixture was stirred for an additional 20 h, then evaporated in vacuo and the resulting residue was purified by column chromatography (20:1 to 12:1 CH_2Cl_2/MeOH gradient) to afford compound **4** (0.05, 0.08 mmol, 57% yield) as an orange solid. mp 178–180 ºC. ^{1}H NMR (400 MHz, CD_3OD) δ 8.60 (d, *J* = 4.5 Hz, 1H), 8.58 (d, *J* = 2.3 Hz, 1H), 8.23 (s, 1H), 8.05 (dd, *J* = 8.9, 2.3 Hz, 1H), 7.91 (d, *J* = 8.6 Hz, 2H), 7.85 (d, *J* = 8.7 Hz, 2H), 7.52–7.41 (m, 2H), 7.40–7.31 (m, 2H), 7.13–7.06 (m, 2H), 6.82 (d, *J* = 8.1 Hz, 1H), 4.09 (dd, *J* = 13.2, 6.3 Hz, 1H), 4.01 (t, *J* = 6.6 Hz, 1H), 3.83 (dd, *J* = 13.2, 6.9 Hz, 1H), 3.71 (t, *J* = 4.6 Hz, 4H), 2.79–2.57 (m, 4H); ^{13}C NMR (100 MHz, CD_3OD) δ 169.5, 166.6, 164.4, 158.5, 155.6, 152.2, 150.1, 149.9, 146.9, 146.8, 138.3, 137.2, 129.3, 128.2, 127.1, 126.9, 125.7, 124.5, 123.5, 123.0, 119.6, 118.6, 116.8, 116.3, 114.3, 70.5, 67.9, 52.0, 41.5; HRMS calculated for $C_{32}H_{32}N_7O_6$: 610.2414 $[M+H]^+$. Found: 610.2393.

(*E*)-N'-(3,4-dihydroxybenzylidene)-2-hydroxy-5-((E)-phenyldiazenyl)benzohydrazide (Dynazo-2)

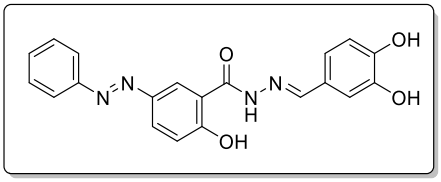

^{1}H NMR (400 MHz, DMSO-d_6) δ 11.95 (bs, 1H), 9.46 (bs, 1H), 9.31 (bs, 1H), 8.54 (d, J = 2.3 Hz, 1H), 8.32 (bs, 1H), 8.00 (dd, J = 8.9, 2.3 Hz, 1H), 7.87 (d, J = 7.4 Hz, 2H), 7.57 (dt, J = 22.5, 7.1 Hz, 3H), 7.28 (d, J = 1.8 Hz, 1H), 7.15 (d, J = 8.9 Hz, 1H), 6.98 (dd, J = 8.1, 1.8 Hz, 1H), 6.81 (d, J = 8.1 Hz, 1H); ^{13}C NMR (100 MHz, DMSO-d_6) δ 163.9, 162.3, 151.9, 149.8, 148.3, 145.8, 144.5, 131.0, 129.4, 126.2, 125.4, 125.4, 122.2, 121.0, 118.5, 116.4, 115.6, 112.8; HRMS calculated for $C_{20}H_{15}N_4O_4$: 375.1093 $[M–H]^-$. Found: 375.1092.

(*E*)-5-((*E*)-(4-acetylphenyl)diazenyl)-*N*'-(3,4-dihydroxybenzylidene)-2-hydroxybenzohydrazide (Dynazo-3)

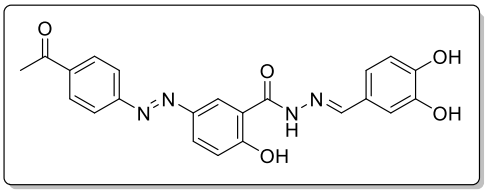

^{1}H NMR (400 MHz, DMSO-d_6) δ 11.90 (bs, J = 9.5 Hz, 1H), 9.46 (bs, 1H), 9.32 (bs, 1H), 8.59 (d, J = 2.4 Hz, 1H), 8.33 (bs, 1H), 8.17 (d, J = 8.6 Hz, 2H), 8.05 (dd, J = 8.9, 2.3 Hz, 1H), 7.97 (d, J = 8.6 Hz, 2H), 7.28 (d, J = 2.0 Hz, 1H), 7.18 (d, J = 8.9 Hz, 1H), 6.99 (dd, J = 8.2, 1.9 Hz, 1H), 6.81 (d, J = 8.1 Hz, 1H), 2.65 (s, 3H).^{13}C NMR (100 MHz, DMSO-d_6) δ 197.3, 163.8, 162.7, 154.4, 149.9, 148.4, 145.8, 144.7, 137.9, 129.6, 126.5, 125.9, 125.4, 122.3, 121.0, 118.5, 116.6, 115.6, 112.8, 26.9; HRMS calculated for $C_{22}H_{17}N_4O_5$: 417.1199 $[M–H]^-$. Found: 417.1196.

1.3. NMR Spectra

^{1}H NMR spectra (400 MHz, DMSO-d_6) of **5**

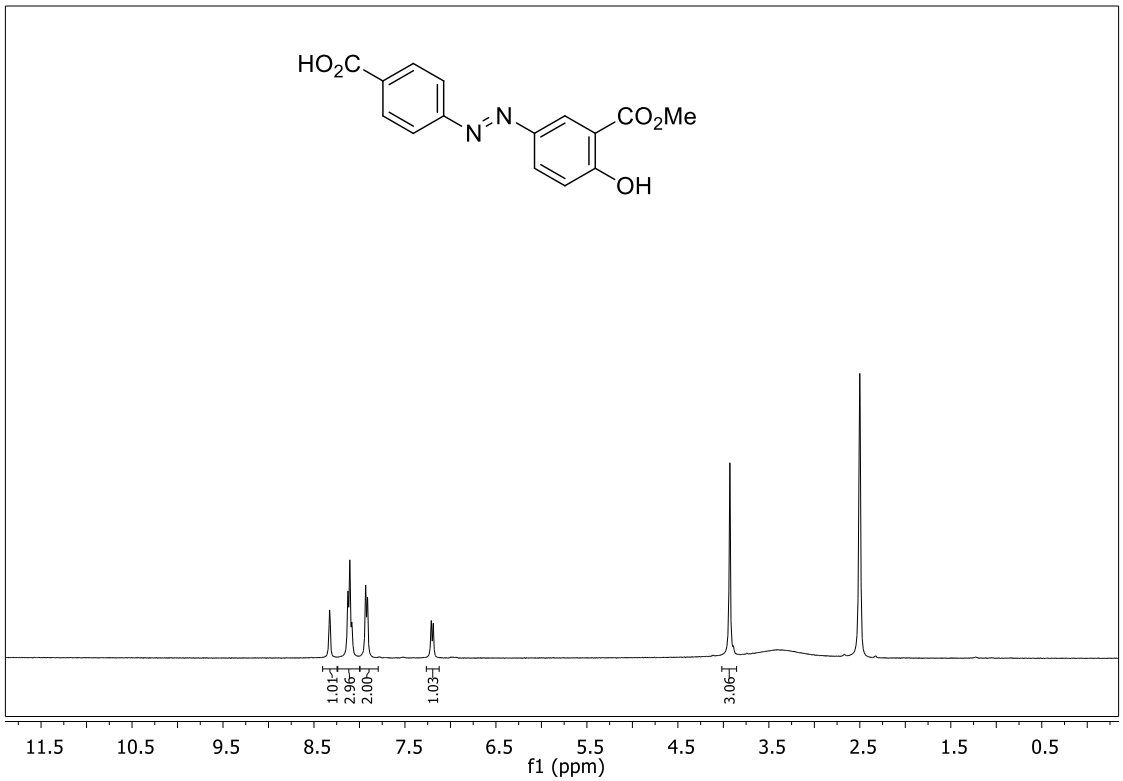

^{13}C NMR spectra (100 MHz, DMSO-d_6) of **5**

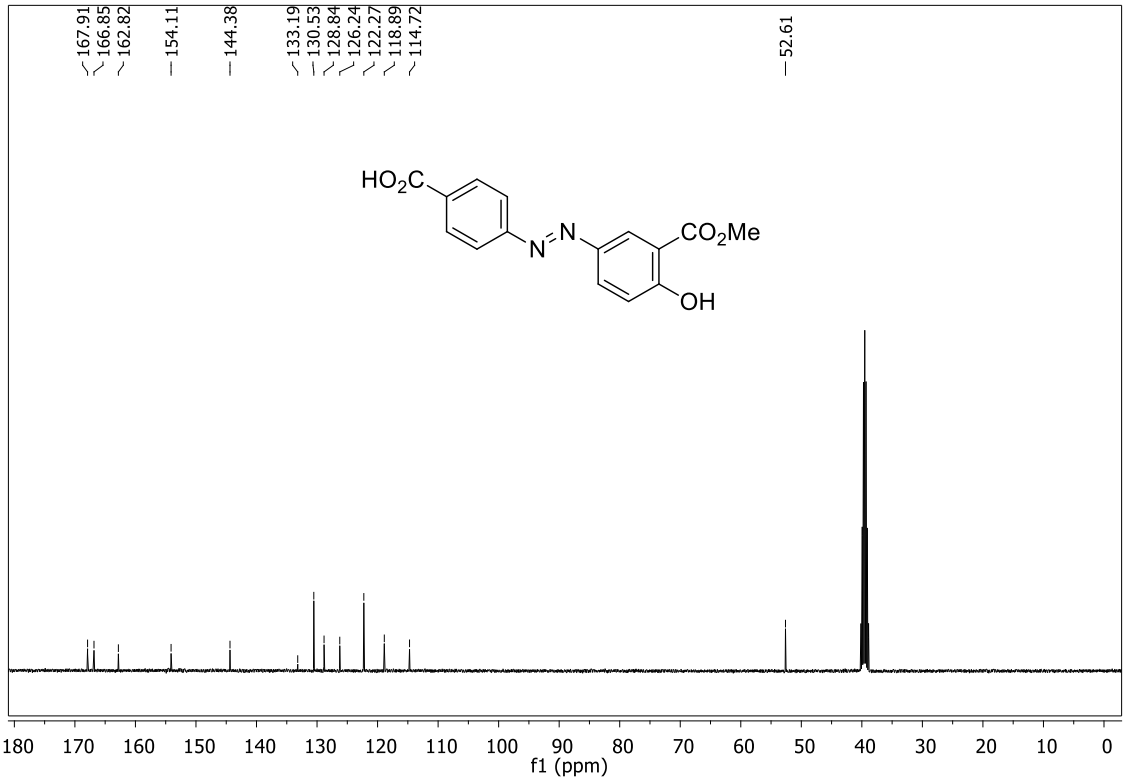

Expansion of ^{1}H-^{1}H gDQCOSY spectra (400 MHz, DMSO-d_6) of **5**

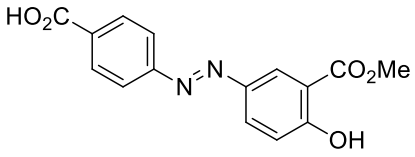

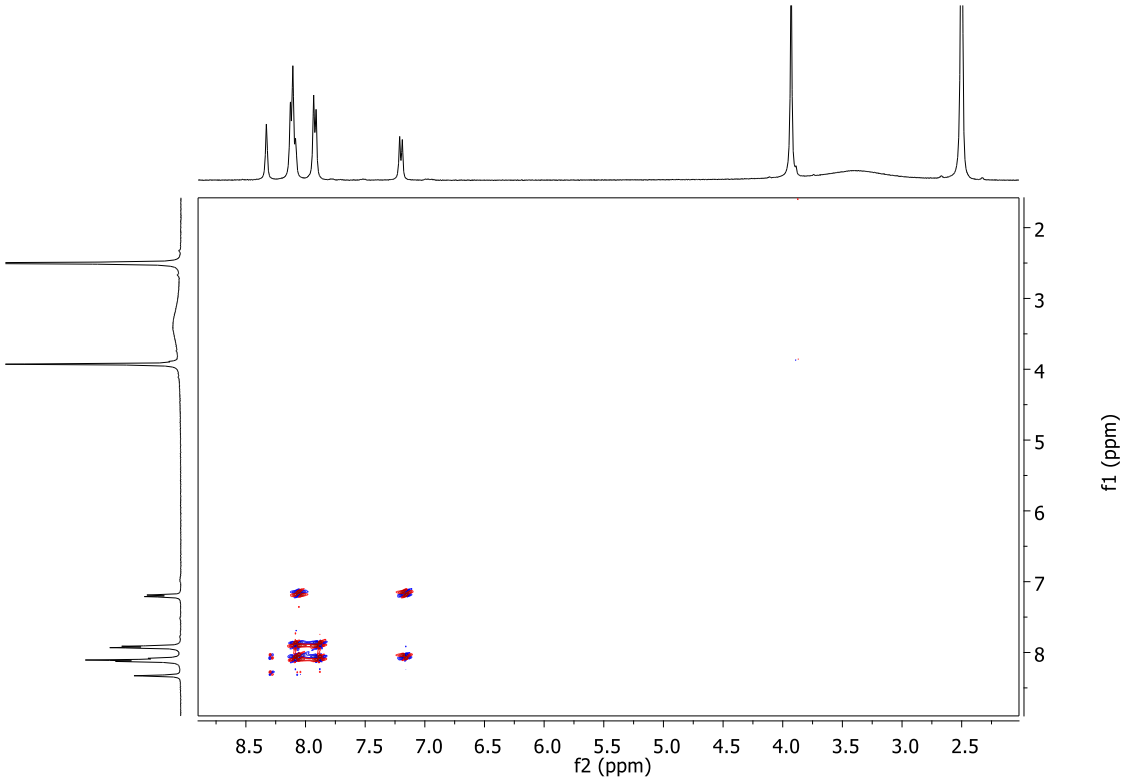

Expansion of ^{1}H-^{13}C gHSQC spectra (400 MHz, DMSO-d_6) of **5**

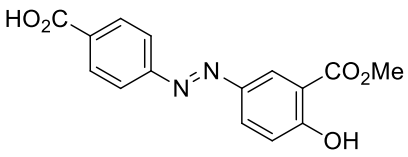

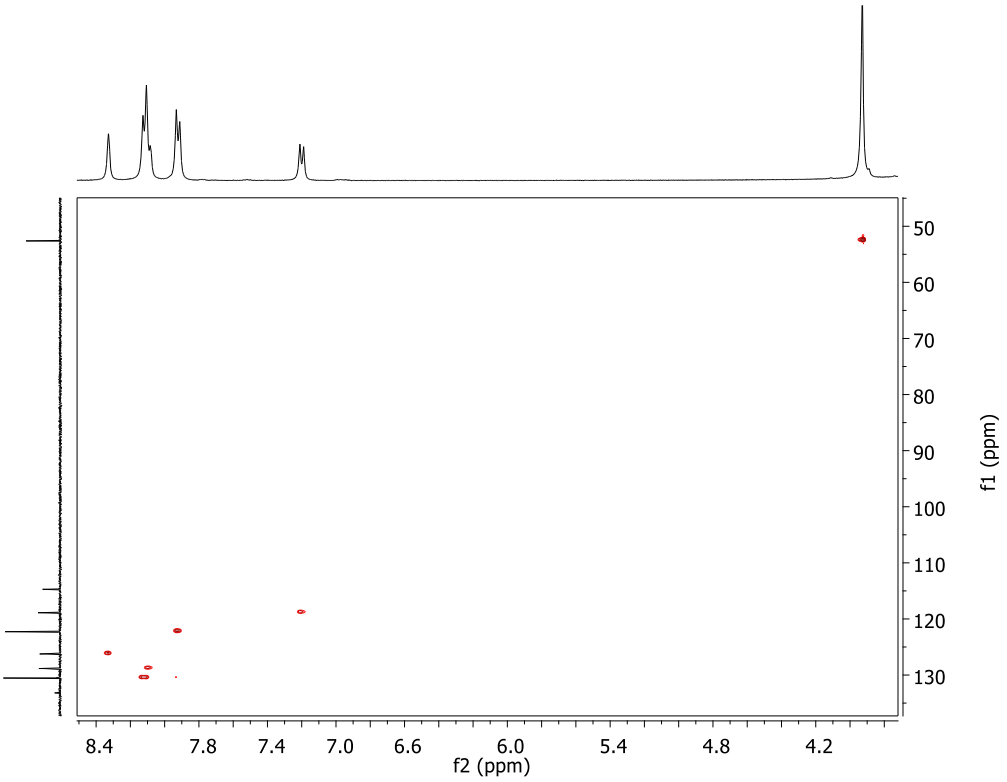

^{1}H NMR spectra (400 MHz, DMSO-d_6) of **6**

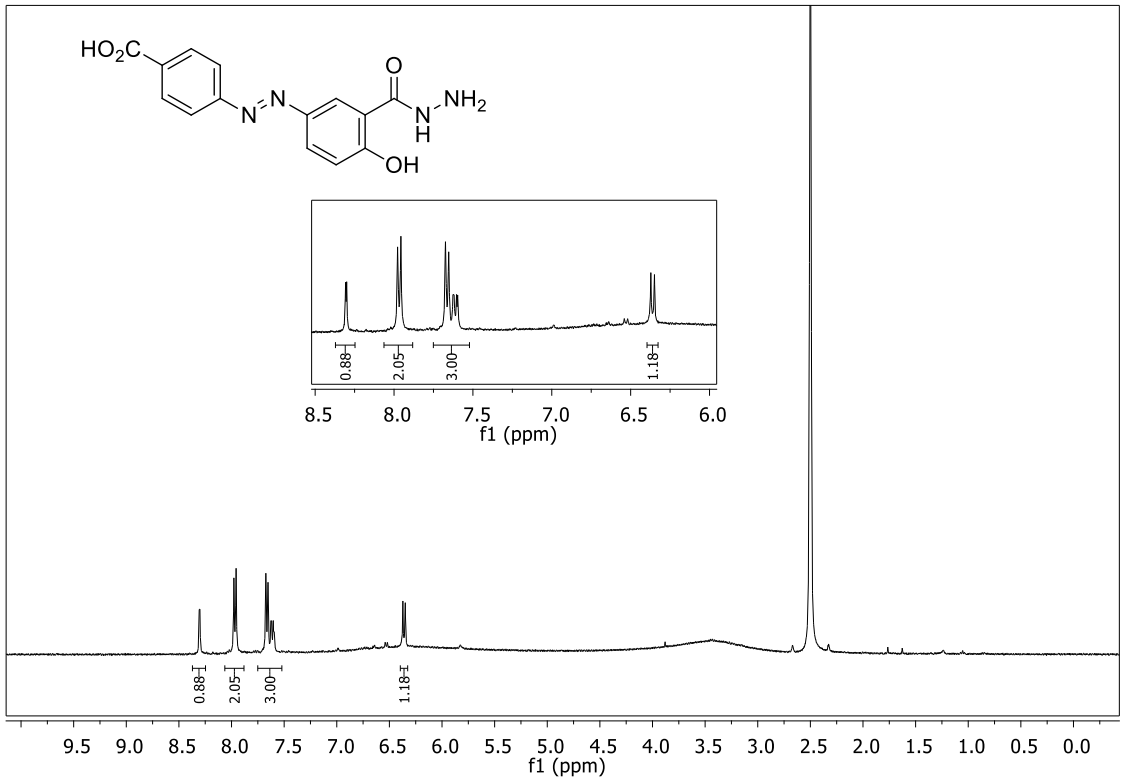

^{13}C NMR spectra (100 MHz, DMSO-d_6) of **6**

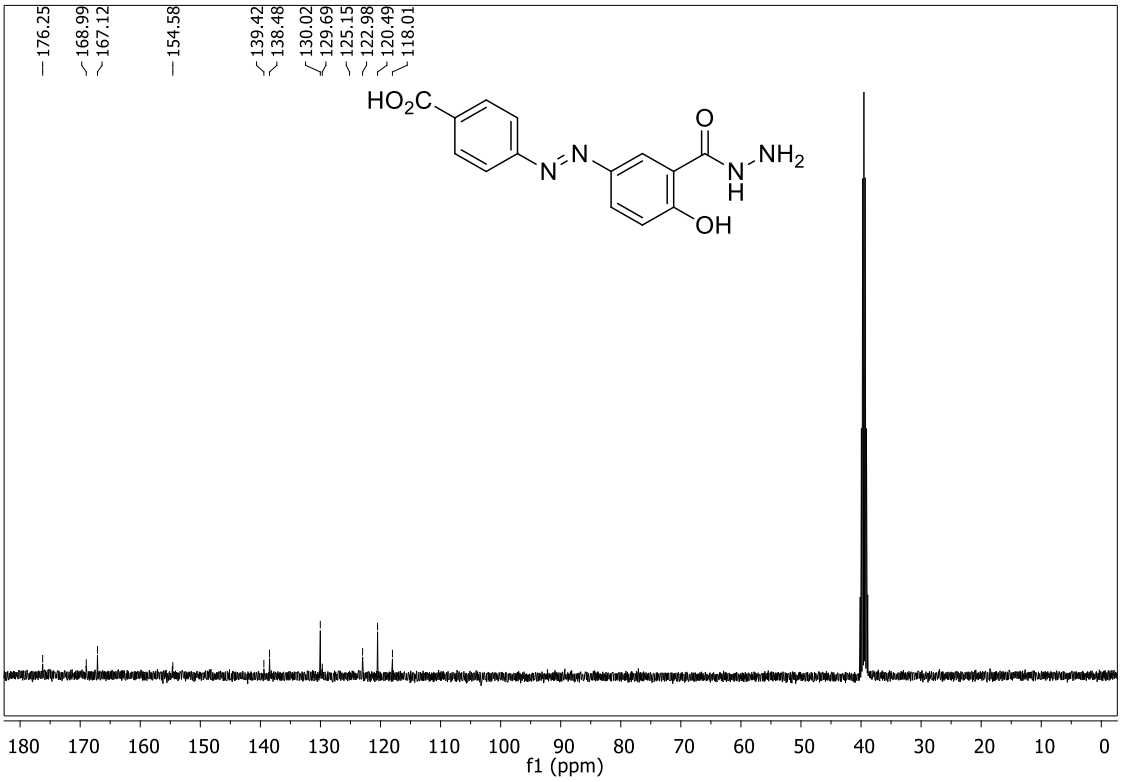

Expansion of ^{1}H-^{1}H gDQCOSY spectra (400 MHz, DMSO-d_6) of **6**

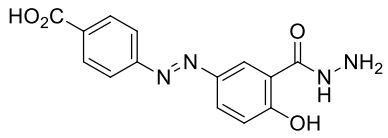

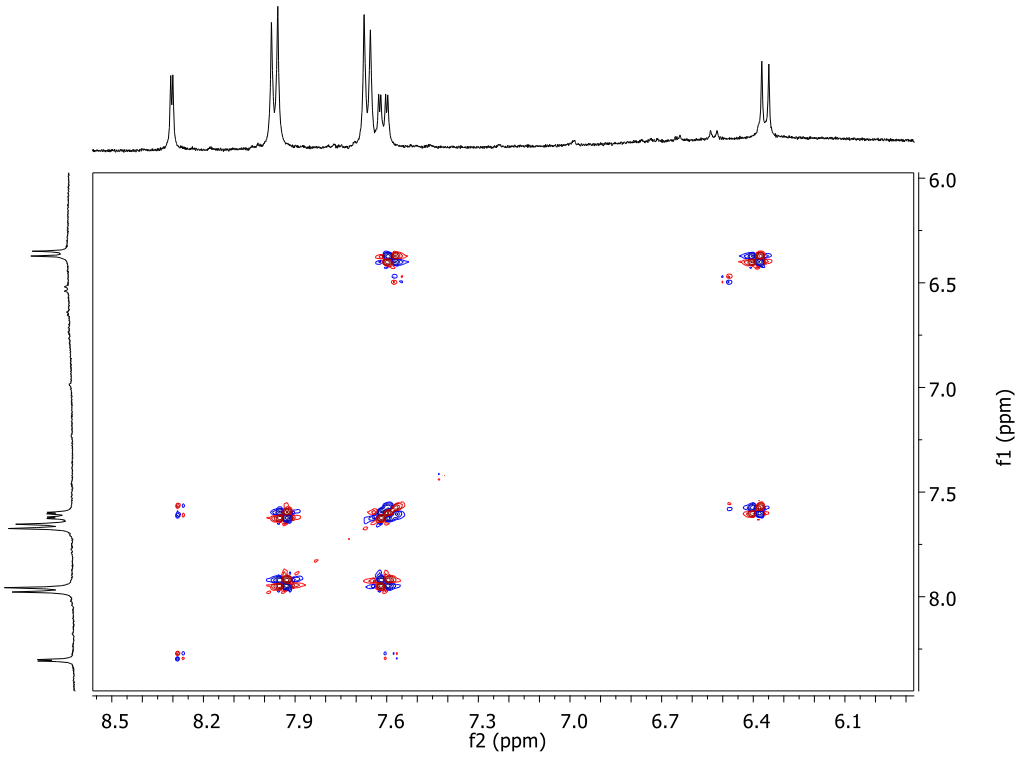

Expansion of ^{1}H-^{13}C gHSQC spectra (400 MHz, DMSO-d_6) of **6**

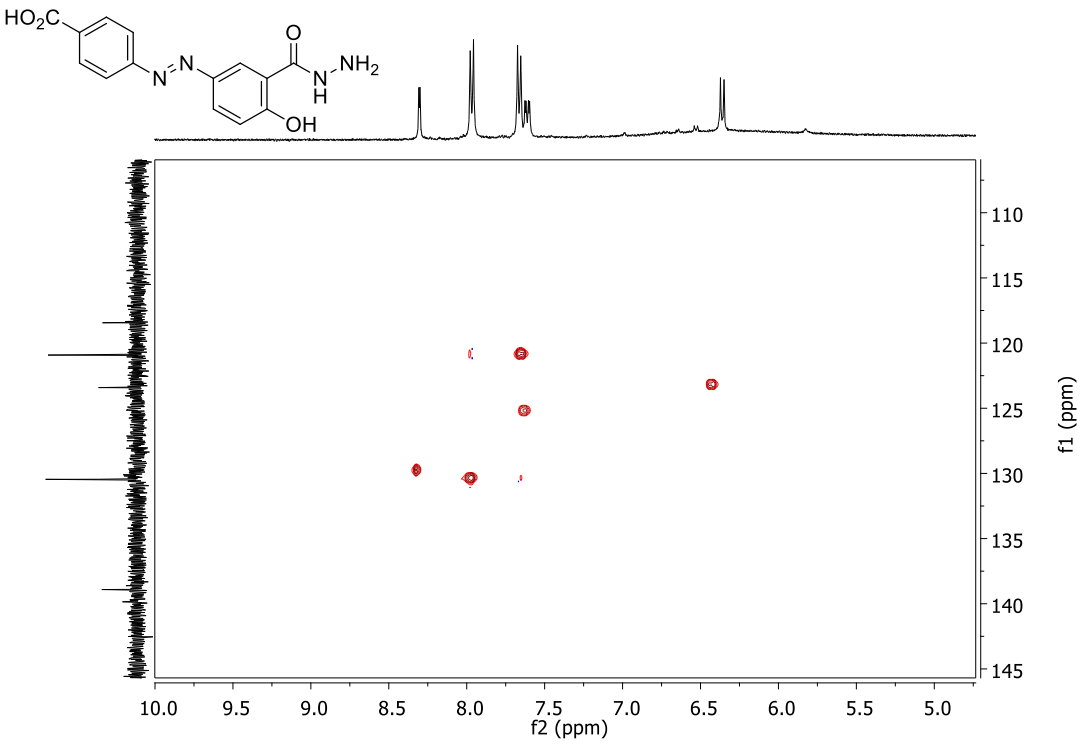

^{1}H NMR spectra (400 MHz, DMSO-d_6) of **7**

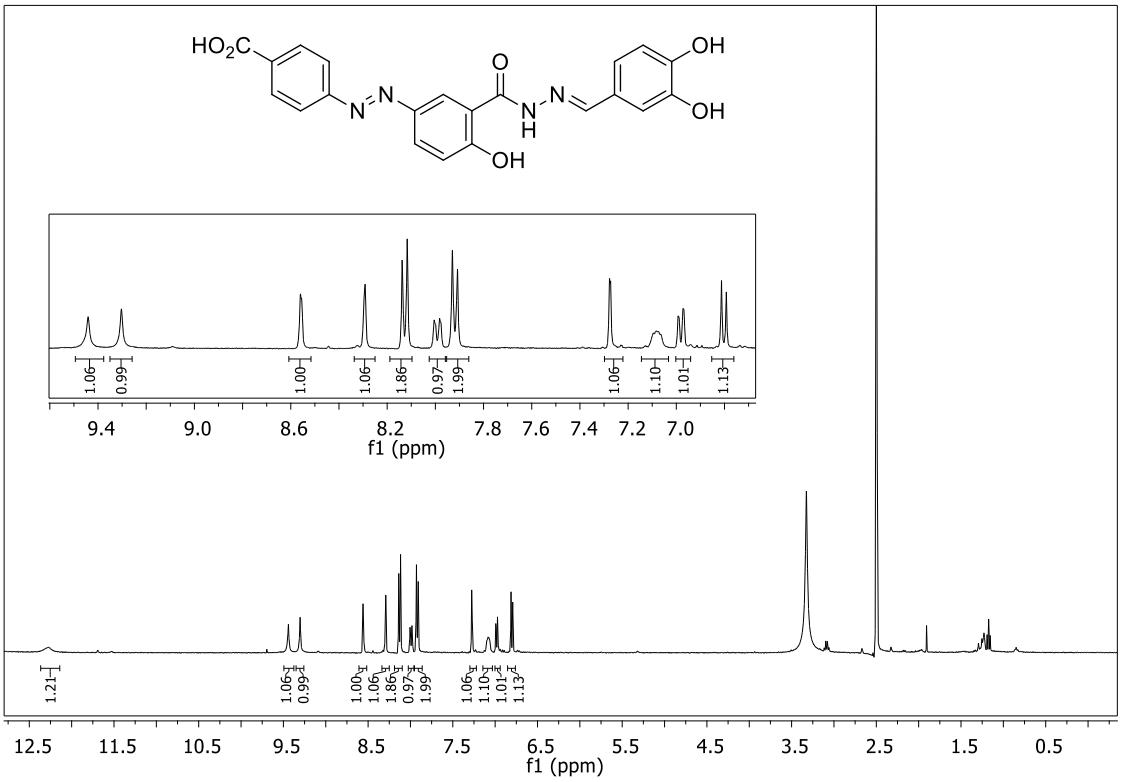

^{13}C NMR spectra (100 MHz, DMSO-d_6) of **7**

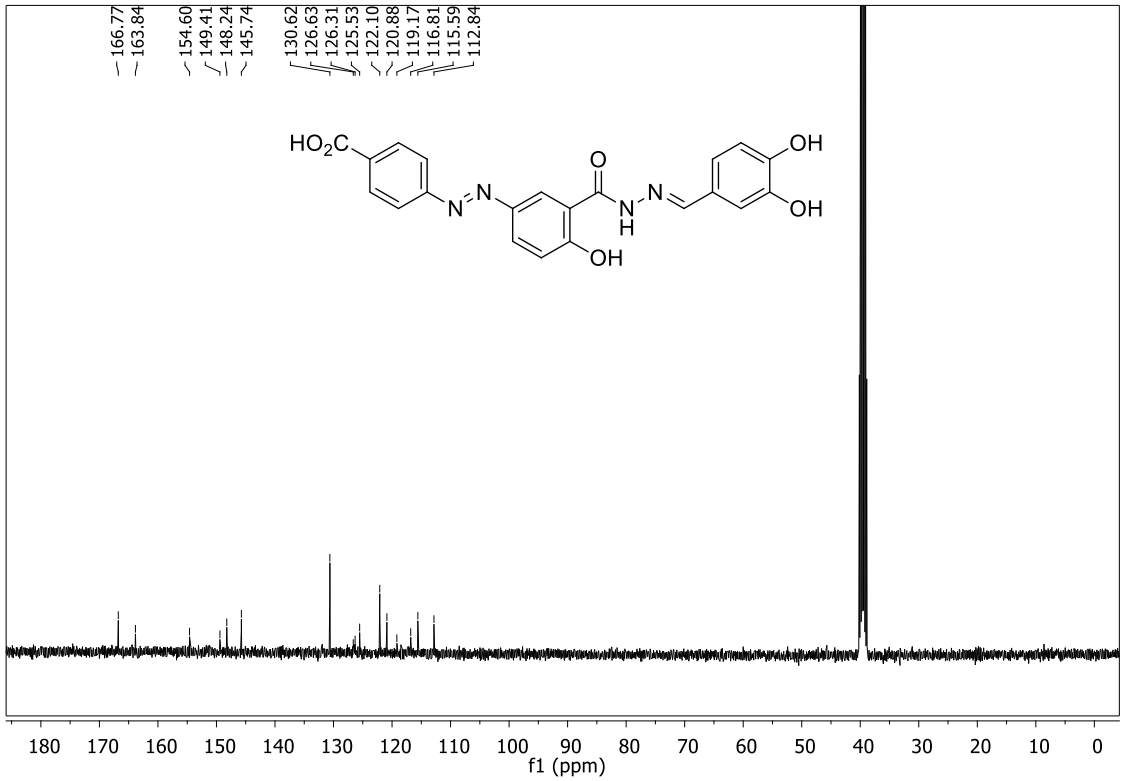

Expansion of ^{1}H-^{1}H gDQCOSY spectra (400 MHz, DMSO-d_6) of **7**

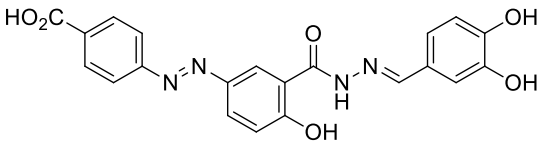

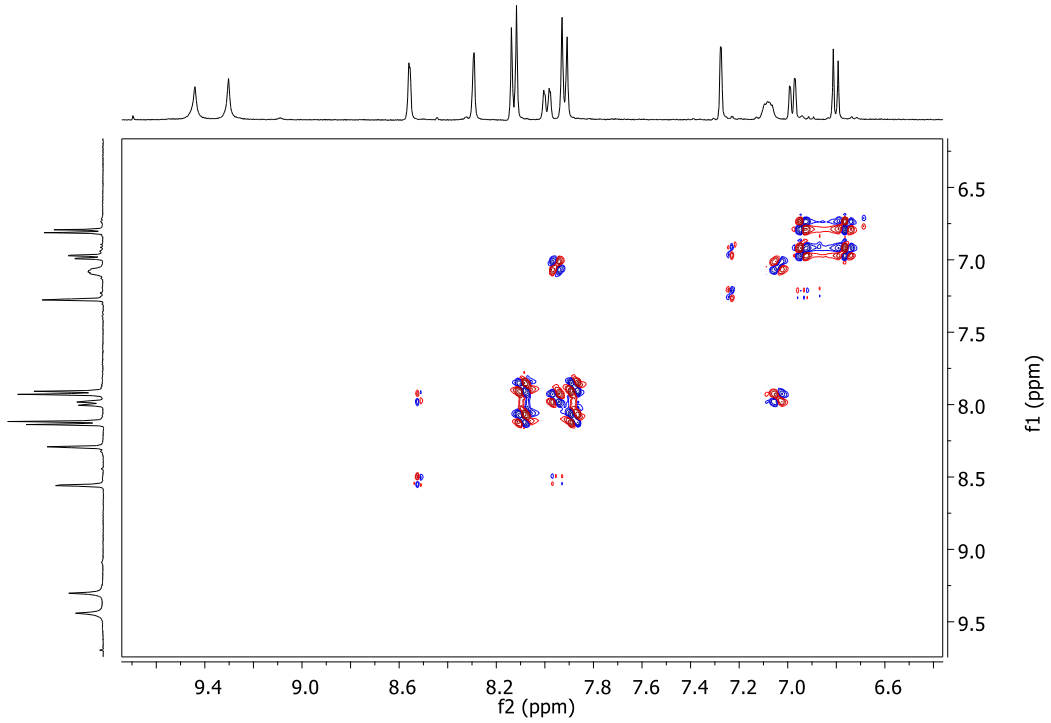

Expansion of ^{1}H-^{13}C gHSQC spectra (400 MHz, DMSO-d_6) of **7**

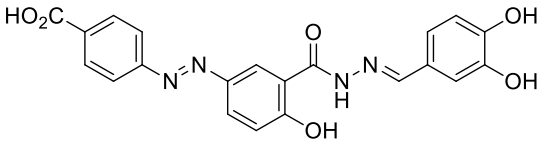

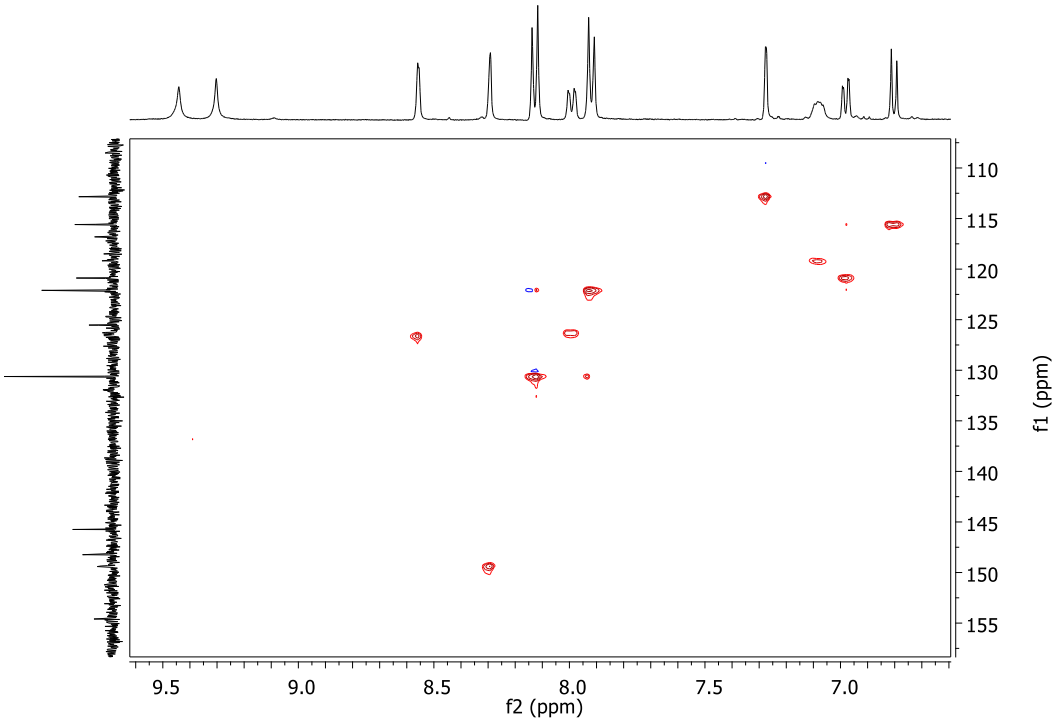

^{1}H NMR spectra (400 MHz, CD_3OD) of **4**

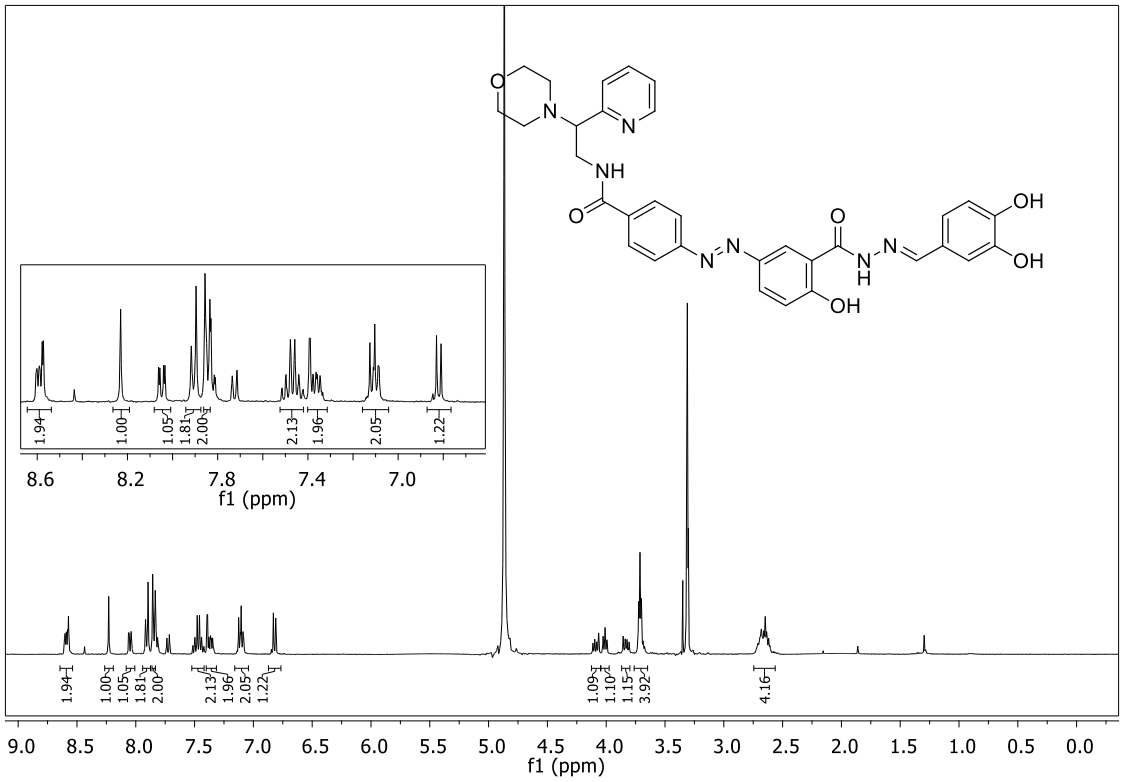

^{13}C NMR spectra (100 MHz, CD_3OD) of **4**

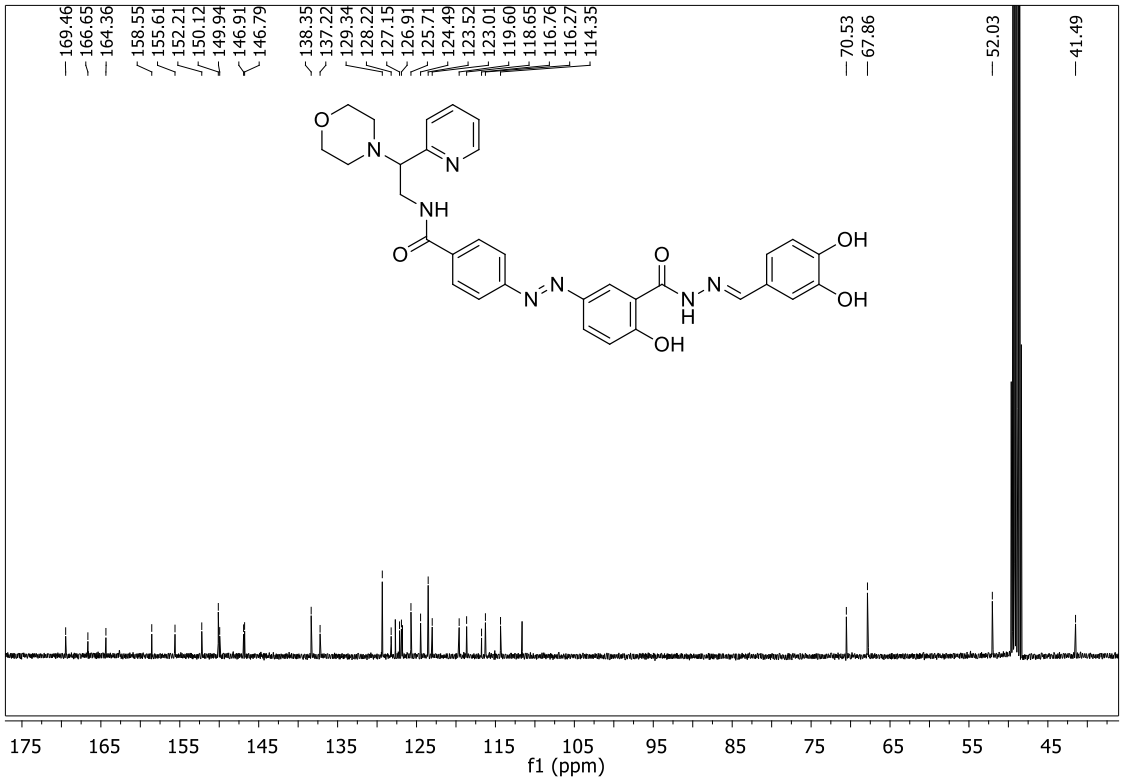

Expansion of ^{1}H-^{1}H gDQCOSY spectra (400 MHz, CD_3OD) of **4**

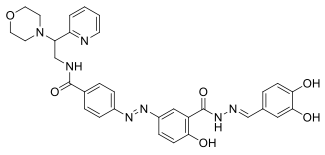

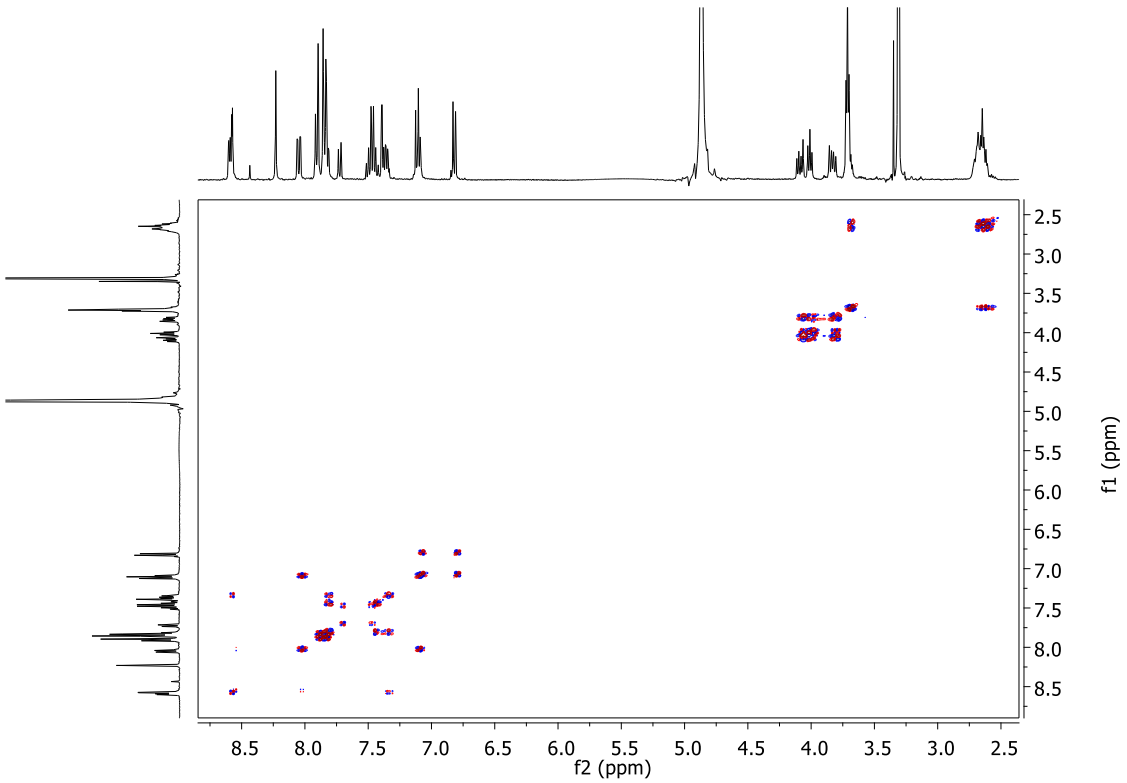

Expansion of ^{1}H-^{13}C gHSQC spectra (400 MHz, CD_3OD) of **4**

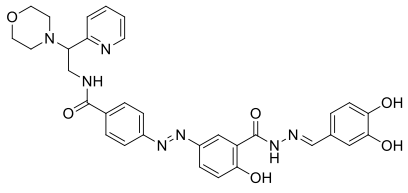

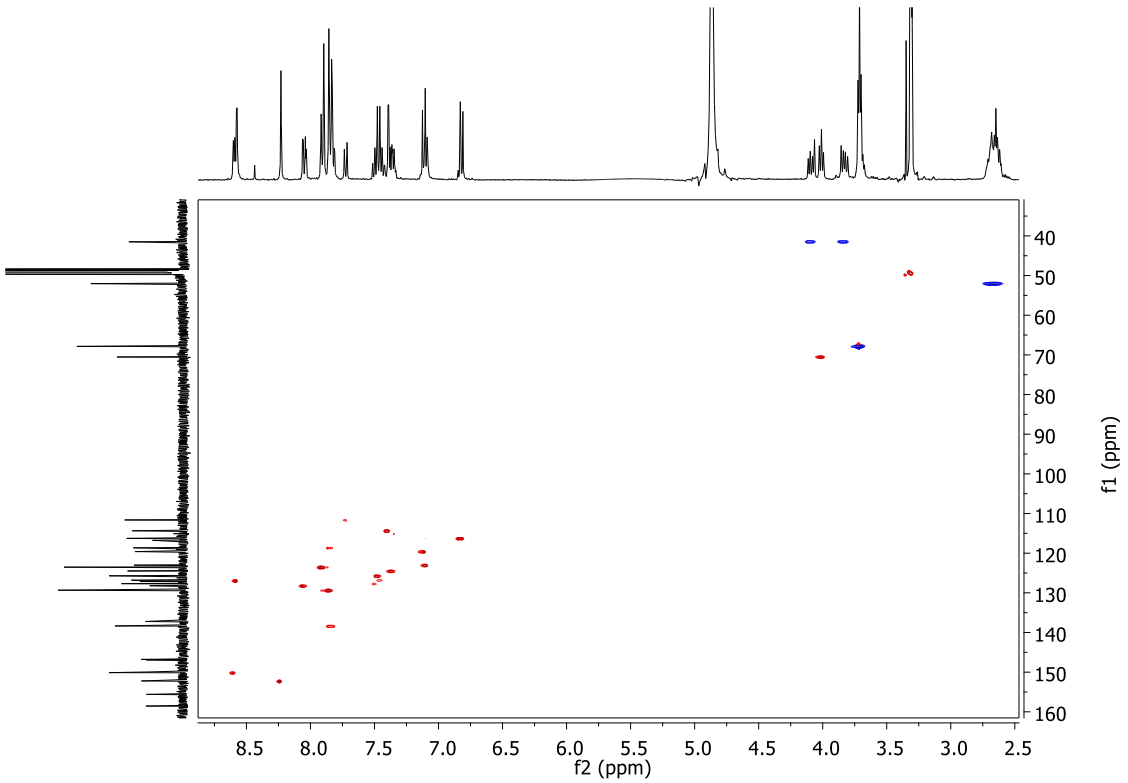

^{1}H NMR spectra (400 MHz, DMSO-d_6) of **2**

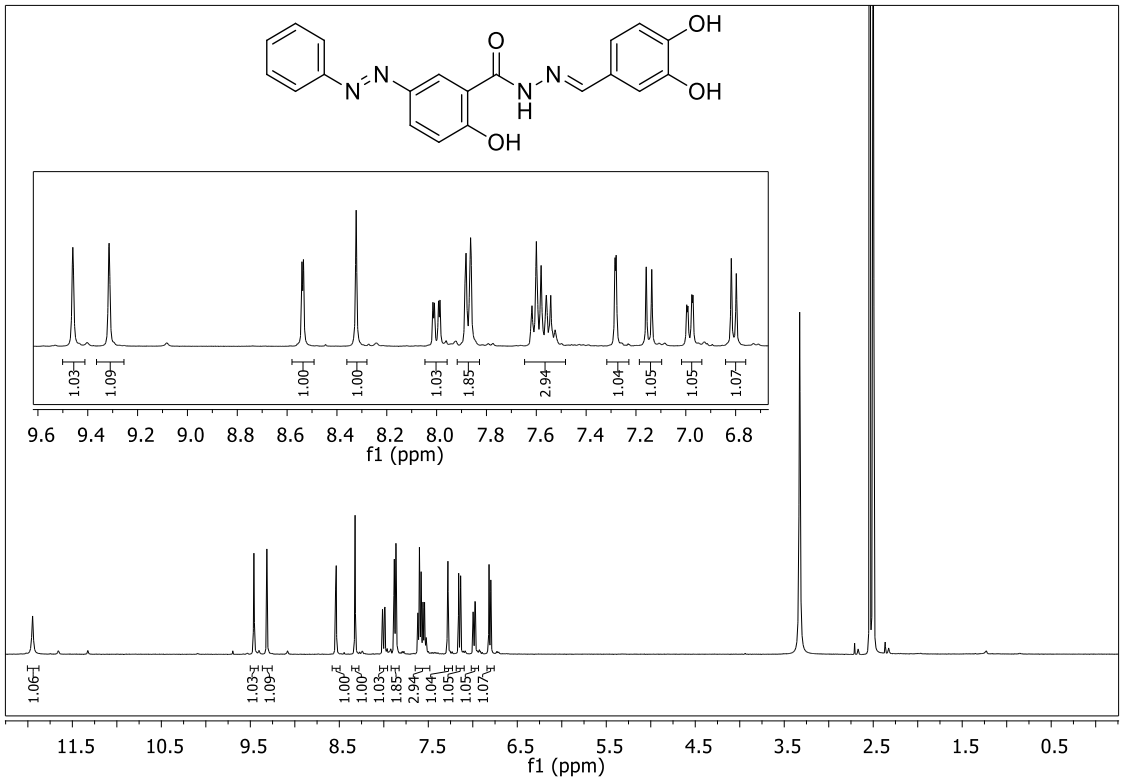

^{13}C NMR spectra (100 MHz, DMSO-d_6) of **2**

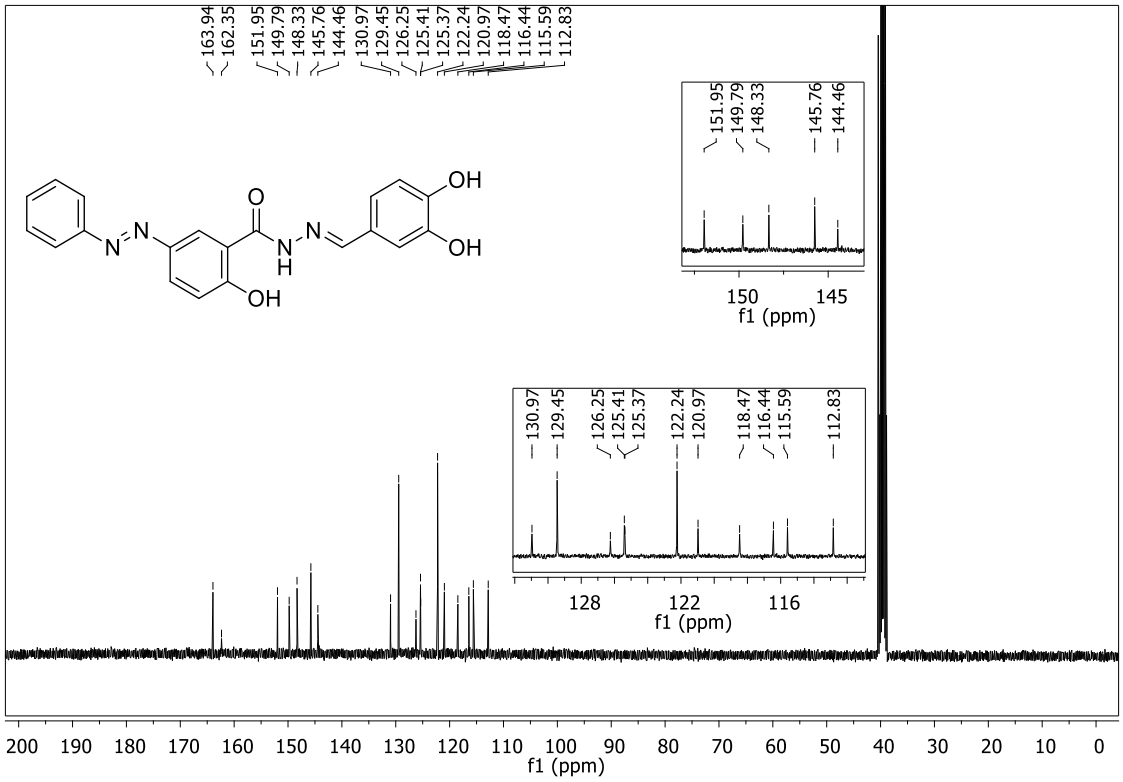

Expansion of ^{1}H-^{1}H gDQCOSY spectra (400 MHz, DMSO-d_6) of **2**

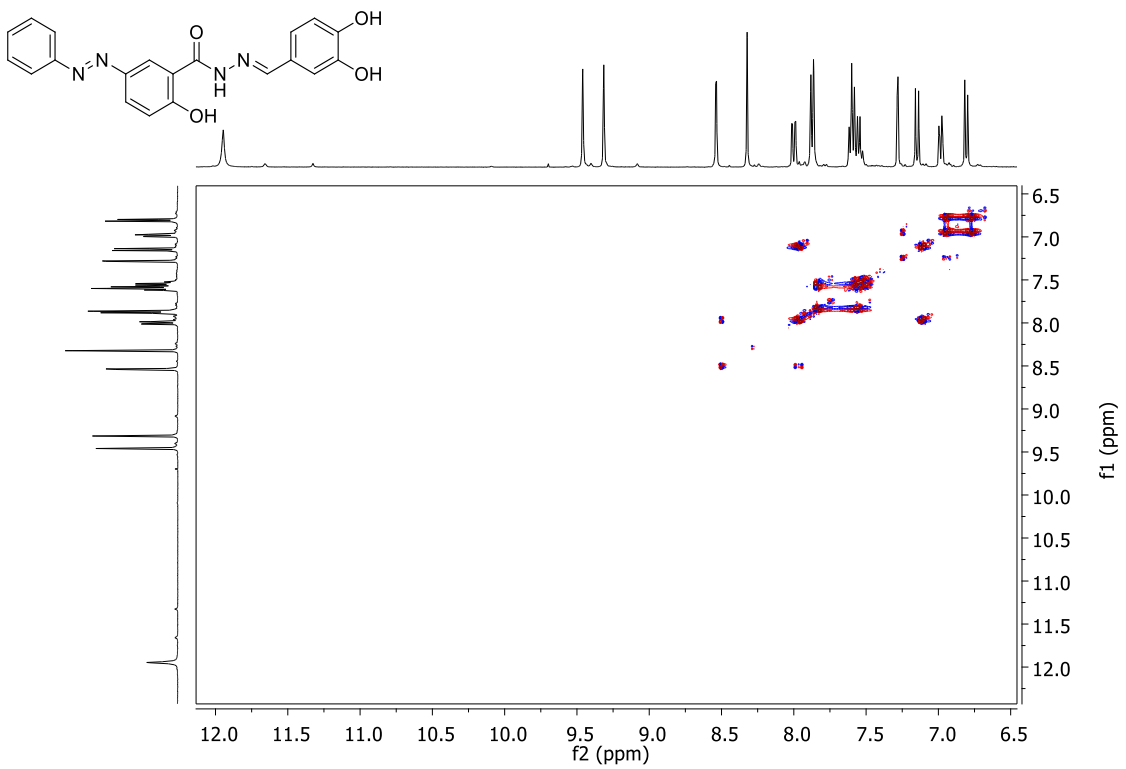

Expansion of ^{1}H-^{13}C gHSQC spectra (400 MHz, DMSO-d_6) of **2**

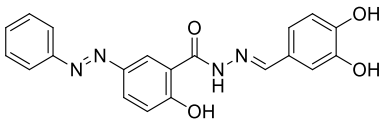

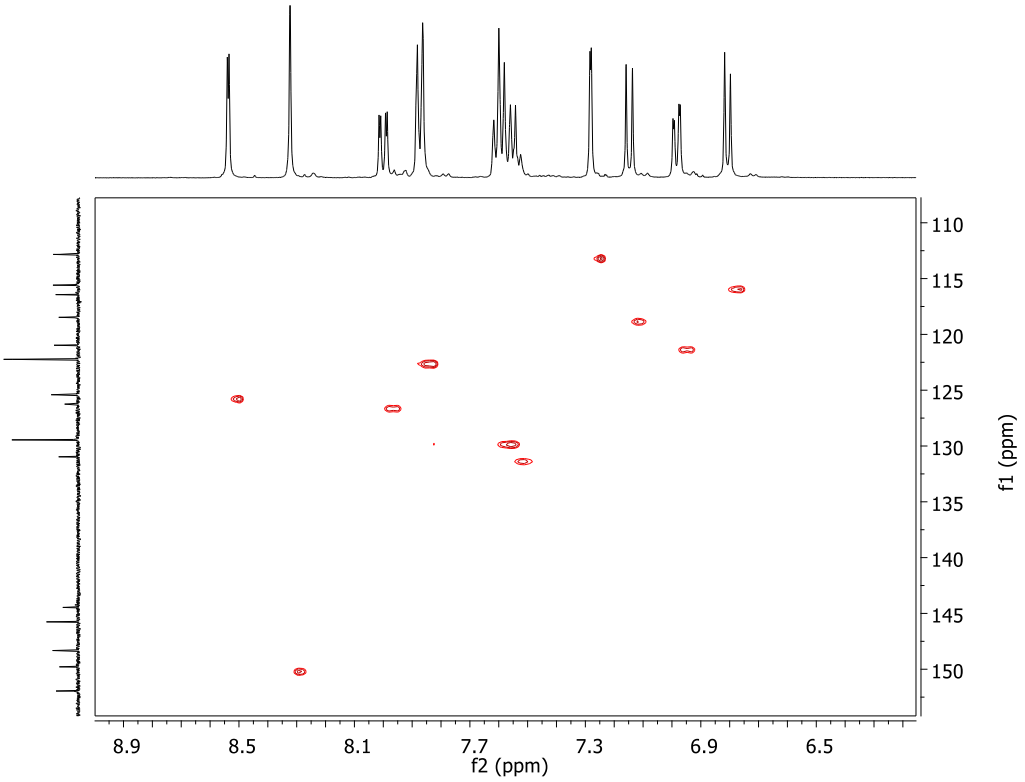

^{1}H NMR spectra (400 MHz, DMSO-d_6) of **3**

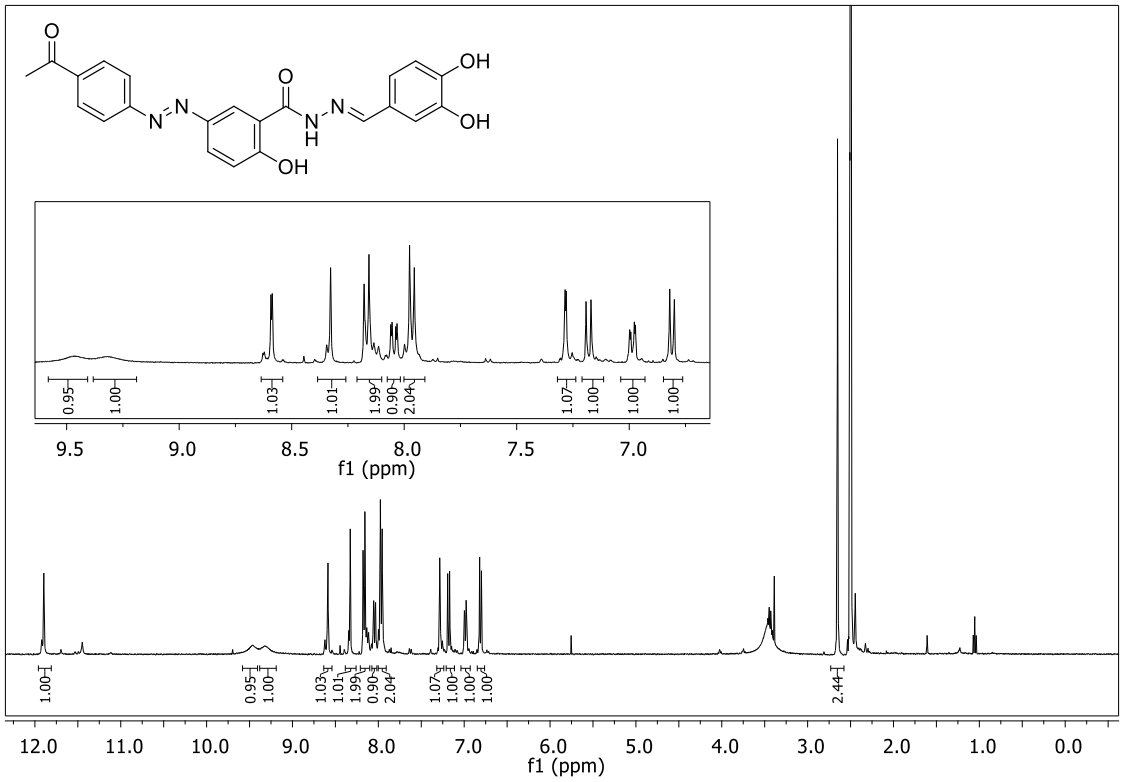

^{13}C NMR spectra (100 MHz, DMSO-d_6) of **3**

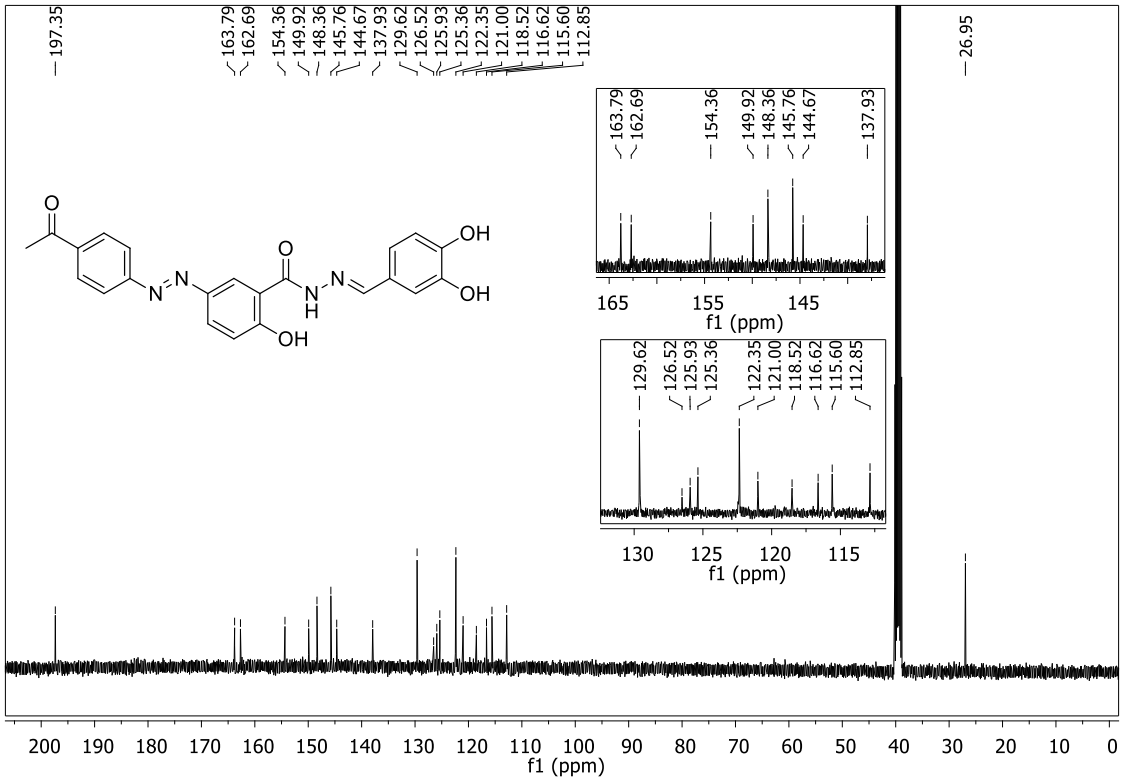

Expansion of ^{1}H-^{1}H gDQCOSY spectra (400 MHz, DMSO-d_6) of **3**

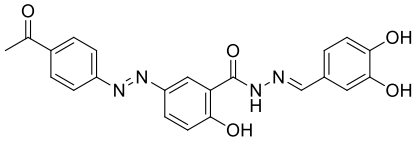

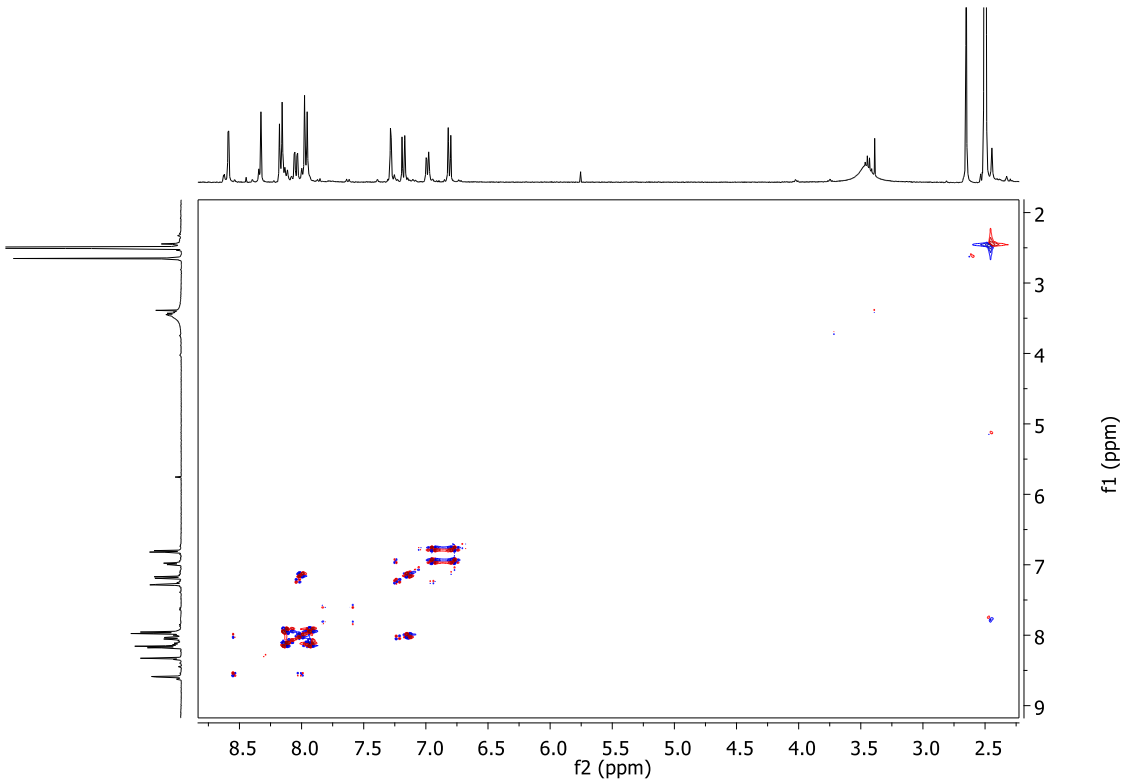

Expansion of ^{1}H-^{13}C gHSQC spectra (400 MHz, DMSO-d_6) of **3**

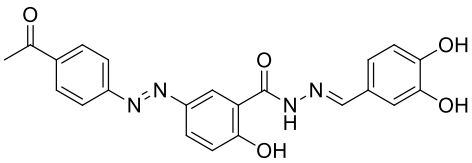

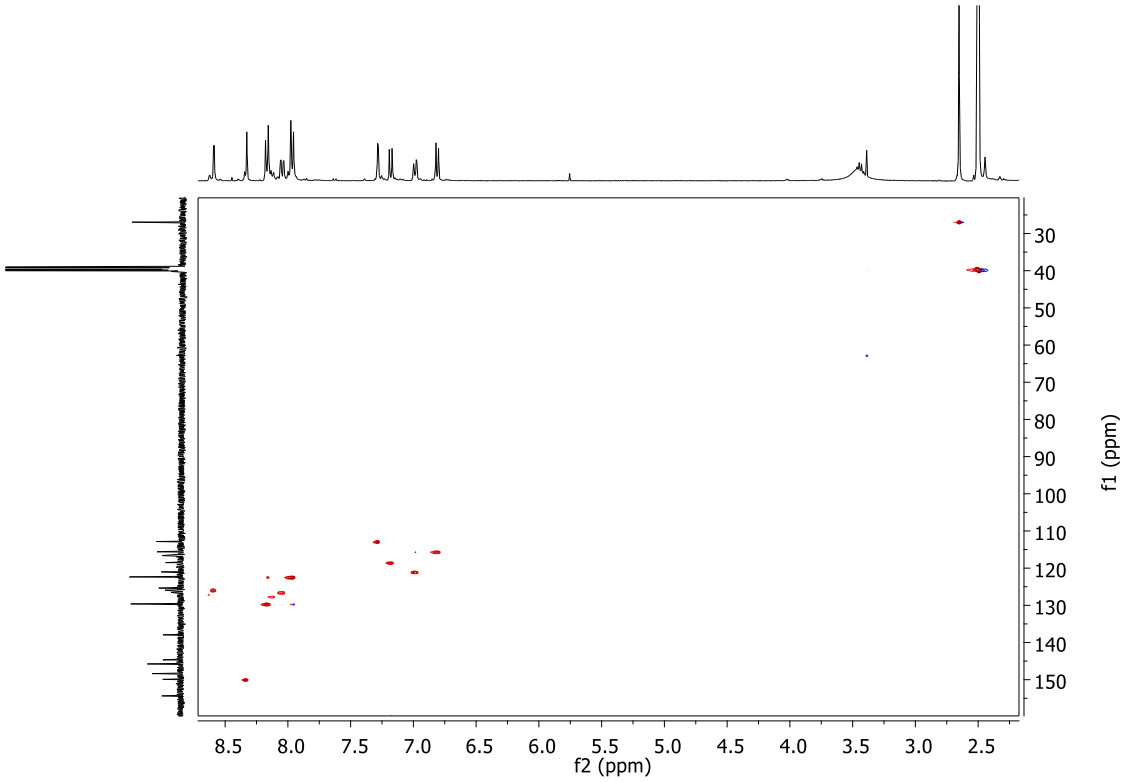

1.4. HPLC Chromatograms

The purity of compound **4** was >94% as determined by HPLC on an Alliance 2695 system with UV detection at 254 nm using a ZORBAX Eclipse Plus C18 (4.6 mm × 75 mm, 3.5 μm) column under the following chromatography conditions: mobile phase A, H_2O with 0.2% HCO_2H; mobile phase B, CH_3CN with 0.2% HCO_2H; flow rate, 1.0 mL min^{-1}; injection volume, 5 μL; elution gradient, 0.0−5.0 min, 5−90% B; 5.0−7.0min, 90% B; 7.0−8.0 min, 90−100% B; 8.0−10.0 min, 100% B; 10.0−11.0 min, 100−5% B; 11.0−15.0 min, 5% B.

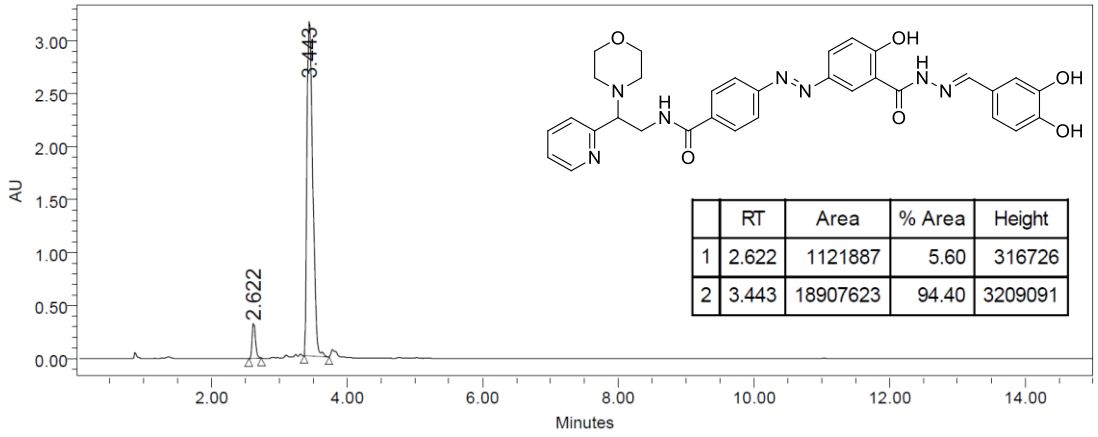

	RT	Area	% Area	Height
1	2.622	1121887	5.60	316726
2	3.443	18907623	94.40	3209091

The purity of compounds **2** and **3** was >96% as determined by HPLC-MS on a Ultimate 3000SD (Thermo Scientific Dionex) coupled to a LTQ XL ESI-ion trap using a ZORBAX Eclipse Plus C18 (4.6 mm × 75 mm, 3.5 μm) column under the following chromatography conditions: mobile phase A, H_2O with 0.05% HCO_2H; mobile phase B, CH_3CN with 0.05% HCO_2H; flow rate, 0.9 mL min^{-1}; injection volume, 5 μL; elution gradient, 0.0−2.0 min, 5% B; 2.0−8.0 min, 5−100% B; 8.0−10.0 min, 100% B; 10.0−11.0 min, 100−5% B; 11.0−15.0 min, 5% B.

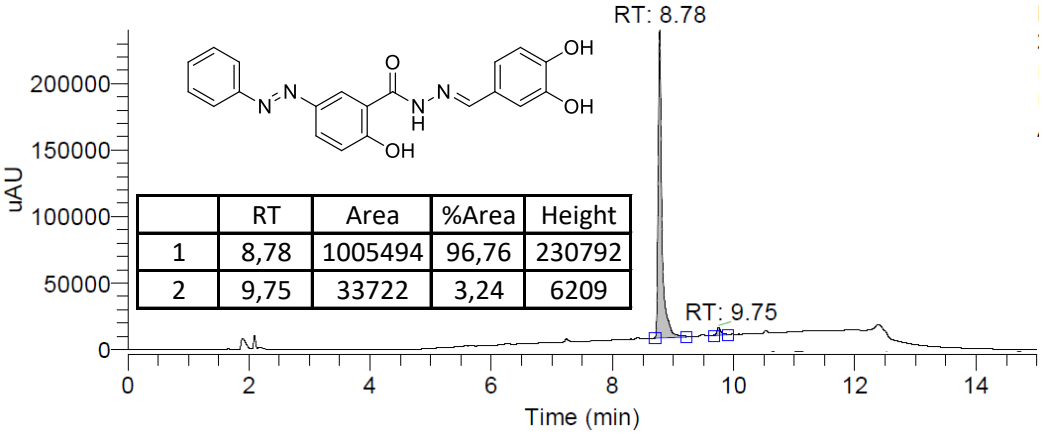

	RT	Area	%Area	Height
1	8,78	1005494	96,76	230792
2	9,75	33722	3,24	6209

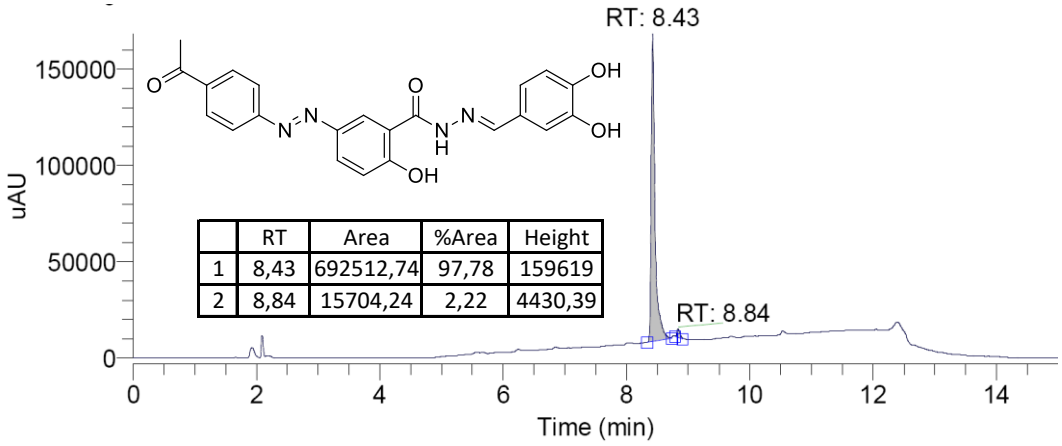

	RT	Area	%Area	Height
1	8,43	692512,74	97,78	159619
2	8,84	15704,24	2,22	4430,39

2. Cell culture.

COS-7 cells were grown in Dulbecco's Modified Eagle Medium: Nutrient Mixture F-12 (DMEM/F12) supplemented with fetal bovine serum (10%), penicillin (100 units mL^{-1}), streptomycin (100 mg mL^{-1}) and L-glutamine (2 mM). Cells were cultured at 37ºC, 5% CO_2 and 95% relative humidity. Dynasore used in cell treatments was purchased from Sigma.

3. Steady state UV-Vis absorption spectroscopy.

Room temperature UV-Vis absorption spectra were recorded in 10 x 10 mm quartz glass cuvettes using a Thermo Scientific Helios gamma UV/Vis spectrophotometer or HP 8453 spectrophotometer. PBS buffer with 1% DMSO content or DMSO were used as solvents.

4. Transient absorption spectroscopy.

Transient absorption measurements were registered in a ns laser flash-photolysis system (LKII, Applied Photophysics) equipped with the third harmonic (355 nm, 2 mJ $pulse^{-1}$) of a Nd:YAG laser (Brilliant, Quantel) as a pump source, a Xe lamp as a probe source and a photomultiplier tube (Hamamatsu) coupled to a spectrograph as a detector. 1-cm thick quartz cuvettes and PBS with 1% DMSO as a solvent were used in these measurements. Dynazo concentrations were selected as to warrant an absorption of 0.3-0.4 at the excitation wavelength.

5. Photodegradation analysis.

Dynasore and dynazo solutions (ca. 2.5 10^{-5} M) in DMSO or PBS with 1% DMSO were irradiated with either the third harmonic of the Nd:YAG laser (355 nm, 20 mW) or a cw violet laser (TLCQ, 405 nm, 20 mW). Photodegradation effects were monitored in time by measuring the UV-vis absorption spectra of the irradiated solutions.

6. Transferrin uptake assays.

For confocal microscopy analysis, COS 7 cells were cultured on glass coverslips (poly-L-lysine treated) at a density of $30x10^3$ cells per cm^2 and cultured overnight to achieve 60% confluency. The culture medium was discarded, and cells were pre-incubated for 30 min at 37ºC under 5% CO_2 with serum free medium containing vehicle (DMSO 1%) or the corresponding concentration of each inhibitor under dark or illumination conditions (active or inactive inhibitor respectively). Cells were then allowed to cool at RT, the medium was removed, and a solution of Alexa labeled Transferrin (A568-Tf, Invitrogen, 20 µg $mL^{-}1$) was added for 2.5 min. This strategy allows the interaction of transferrin with the receptor but slows down internalization. Afterward, the medium was discarded and the inhibitor containing medium was re-added, while promoting internalization at 37ºC for 15 min, again under dark or illumination conditions. Internalization was stopped by chilling the cells on ice. Finally, cells were acid washed twice (0.15M NaCl, 0.1M Glycine pH 2.8) to remove surface-bound transferrin, washed with PBS and fixed in 4% formaldehyde for 15 minutes. Nuclei were counterstained using DRAQ5 dye (Thermo Scientific). Coverslips were mounted in glass slides and images were acquired with a laser scanning confocal microscope (Leica TCS-SL), using a 63x oil immersion objective. For each cell, a series of confocal sections images were acquired every 0.3 µm. The integrated projected fluorescence of at least 100 cells for each condition was quantified using Fiji software. To normalize between images, the fluorescence intensity of the vehicle control conditions was set at 100%.

For FACS analysis, COS7 cells were seeded on plastic into 6-wells plates. Inhibitor treatment, protocol of illumination, transferrin incubation and washing were done as described above, except for the use of A488-Tf (Invitrogen, 20 µg mL^{-1}) and the trypsinization of cells after the acidic wash. Trypsinized cells were collected by centrifugation at 4 ºC, resuspended in complete media and kept on ice. Before flow cytometric analysis, propidium iodide was added to the cell suspension for sorting

of living cells. Fluorescence intensity of internalized transferrin was measured for 10000 living cells by flow cytometry using a FACsCanto cytometer (BD Biosciences).

Illumination of inhibitor treated cells was done using a 380 nm and 405 nm custom-made multi-LED lamp (FC Tècnics, Barcelona) placed at 5 cm above the cell preparation, with a light intensity of 0.5 and 1mW cm^{-2} respectively. The light intensities were measured with an optical power meter (1916-C, Newport). For the measurements conducted in the dark, plates of cells were covered with aluminum foil or an IR Transmitting Plastic Sheet (IR780C, Visualplas) that blocks transmission of visible light between 300-700 nm but is transparent to 800-1100 nm IR light.

To study the kinetics of transferrin uptake in untreated COS-7 cells we used the above-described protocol, but incubating cells at 37 ºC for the indicated times and followed by immediate cooling on ice to arrest internalization. Internalized Tf at each time is expressed as the percentage of the initial total surface bound Tf (100%).

7. TIRF microscopy.

In order to track microscopic endocytic events in real time, we used live-cell total internal reflection fluorescence microscopy (TIRFM) (Mettlen and Danuser, *Cold Spring Harb Perspect Biol*. 2014;6(12):a017038), and assessed the capacity of dynazo-4 to photocontrol the dynamics of clathrin-coated pits (CCP) formation in cells expressing the eGFP-tagged adaptor protein AP-2. We used the BSC1 monkey kidney epithelial cell line stably expressing the σ2-AP-2 -EGFP fusion kindly provided by Dr. T. Kirchhausen, Harvard Medical School. BSC1 cells were plated on poly-L-lysine treated glass coverslips (#1.5, 23 mm diameter, round) and cultured overnight to achieve 60% confluency. The culture medium was discarded, cells were washed, and coverslips were then mounted on an Attofluor Cell Chamber (Thermo Scientific) in imaging medium (DMEM, devoid of phenol red and FBS). For imaging, the mounted cells were rapidly transferred to a prewarmed microscope stage (37°C and 5% CO_2). To prevent medium evaporation during the experiments, the chamber was

covered with a Foil cover ring containing a membrane CultFoil (25 µm). Live-cell microscopy was performed using an inverted TIRF microscopy (Olympus) with a 100x/1.45NA oil PlanApo objective, under the control of Xcellence Software. Movies were recorded using a 12-bit Hamamatsu Orca-ER camera at 0.5 Hz for 2 minutes each. After the recording of CCP dynamics in control conditions, 25 µM dynazo-**4** was added dropwise with a home-made perfusion system inside the microscope, and cells were incubated for 40 minutes before starting the recording again. Illumination in the presence of the dynazo-**4** was performed with the multi-LED plate system mentioned above. The plate was directly introduced and retained in the microscope cabin —located above the cell preparation— during the whole experiment.

Detection of the number of events and quantification of the CCP lifetimes was performed on TIRFM images with a section area of 1600 µm^2. Images analysis and CCP tracking was performed with ImageJ[1] (http://imagej.nih.gov/ij/) using a custom written software as described previously. [2] Briefly, background and noise were reduced by applying a 2D Laplacian filter, followed by a pass of rolling ball. Detection and tracking of the spots were done with the help of the "Particle tracker" ImageJ plugin implementing the described algorithm.[3] For each movie, the parameters of the algorithm were adjusted by the experimenter to ensure the best apparent tracking results: rejection of spurious detections, single hit for most apparent spots, and robust track linking. An ImageJ macro was used to automate the pre-filtering and the extraction of the CCP time duration from the results of the automatic tracking. Tracks included in the analysis were filtered of short-lived nonproductive CCP (< 20 s). These results are shown in the new Suppl. Figures 6, 7, and 8. TIRFM experiments revealed a significant increase in the mean lifetime of the CCP detected after dynazo-4 treatment and an increasing trend in the number of CCP detected, indicating a slowdown of the endocytic process that is in full agreement with Tf uptake assays by cytometry and fluorescence microscopy (Fig. 3). 405 nm illumination can revert this effect at times ≥ 2 min, probably due to the fast relaxation lifetime of dynazo-4, which limits the effective % of (inactive) *cis* isomer that can be achieved under illumination.

Previous studies have shown that alteration of dynamin activity through dynasore treatment or RNAi dynamin knockdown increased the mean lifetime of CCP and that these changes affected differentially the short and long-lived CCP subpopulations (see *Nat Methods*. 2008;5(8):695-702 and *PLoS Biol*. 2009 Mar 17;7(3):e57). Analysis of the relative percentages of CCP subpopulations in TIRF experiments shown in Supplementary fig. 7c, revealed a significant decrease in the most abundant CCP pool (time duration between 20-40 seconds, 60% of the CCP detected) and a significant increase in the long-lived CCP pool (time duration ≥120 s, negligible in the control condition). 405 nm illumination could revert this effect over the CCP subpopulation with a time duration of ≥120 s. These results can be attributed to the differential recruitment of dynamin during the formation of non-productive CCP (dynamin negative) and productive CCP (dynamin positive) subpopulations. It has been stablished that early dynamin recruitment is a prerequisite for the formation of a productive CCP (see Aguet *et al*, *Dev Cell* 2013, 26(3), 279–291).

7. Supporting Figures

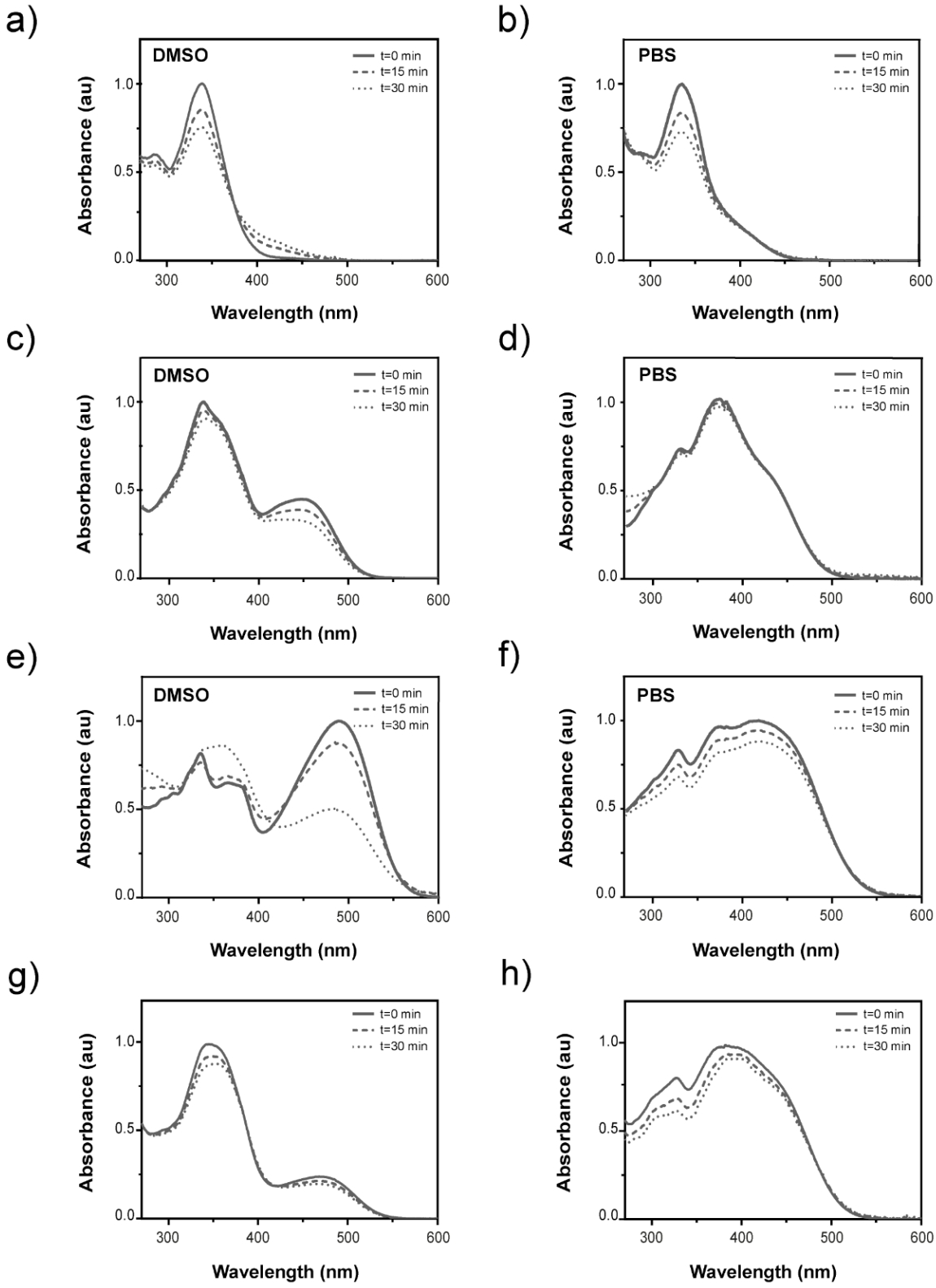

Supplementary Figure 1. Spectral changes in the UV-vis absorption spectra of (a-b) dynasore, (c-d) dynazo-2, **(**e-f) dynazo-3 and (g-h) dynazo-4 upon continuous direct excitation with UV light (355 nm, 20 mW, t=minutes) in DMSO (left) or PBS with 1% DMSO (right) respectively.

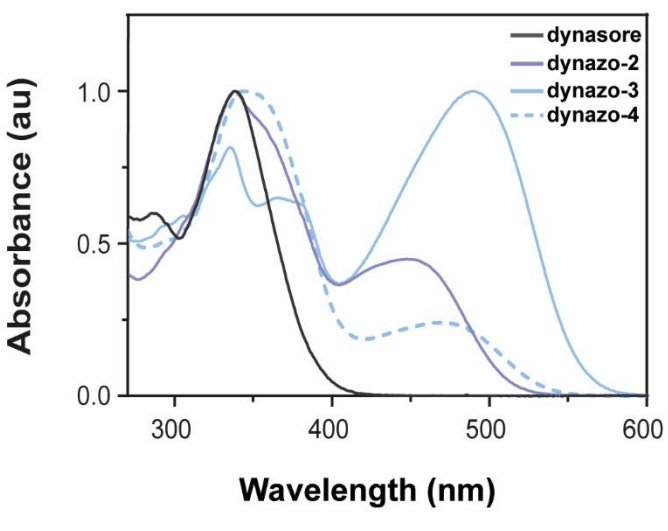

Supplementary Figure 2. UV/Vis absorption spectra of dynasore and dynazos at room temperature in DMSO.

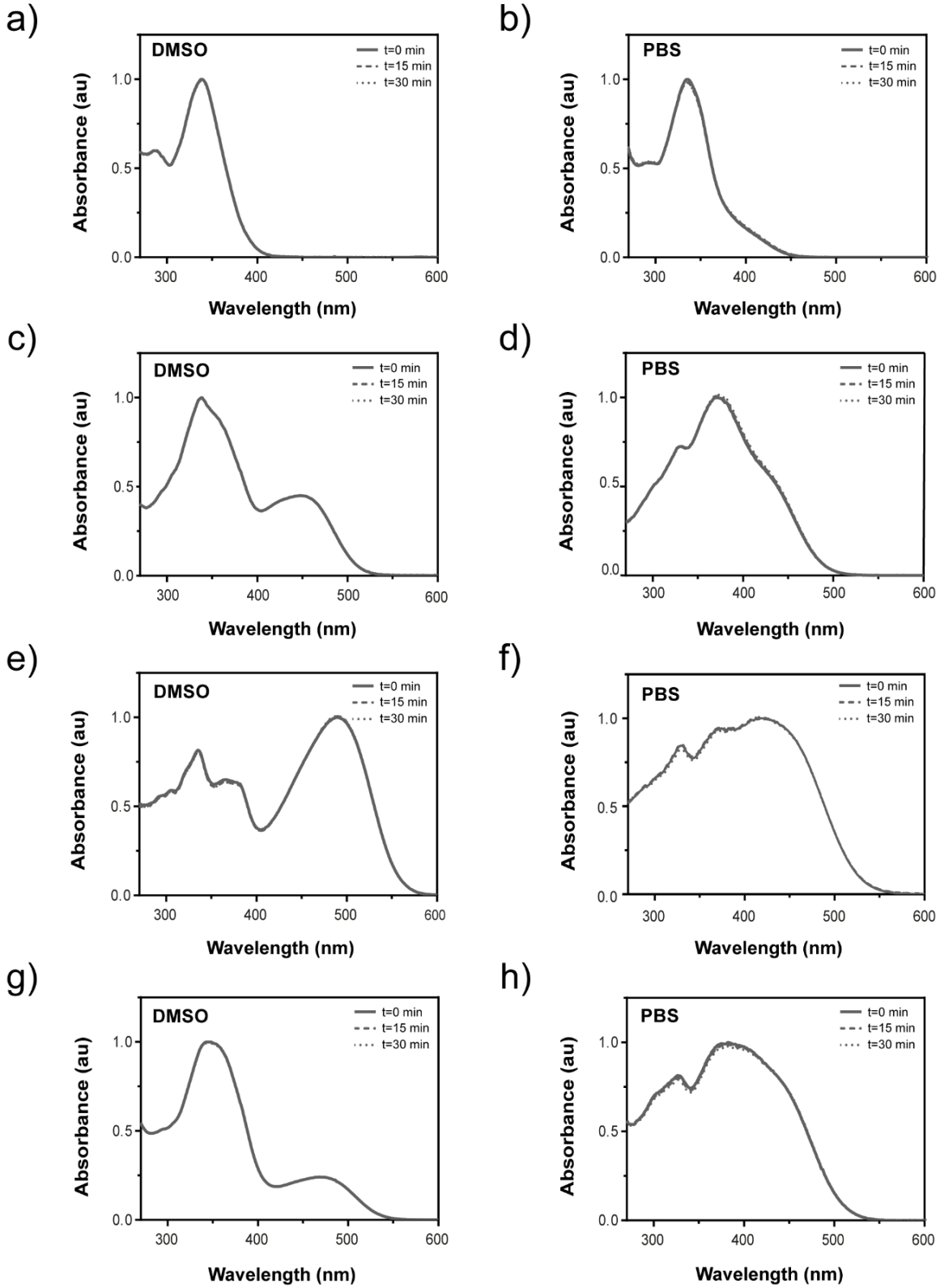
a)
DMSO
t=0 min
t=15 min
t=30 min
Absorbance (au)
Wavelength (nm)
b)
PBS
t=0 min
t=15 min
t=30 min
Absorbance (au)
Wavelength (nm)
c)
DMSO
t=0 min
t=15 min
t=30 min
Absorbance (au)
Wavelength (nm)
d)
PBS
t=0 min
t=15 min
t=30 min
Absorbance (au)
Wavelength (nm)
e)
DMSO
t=0 min
t=15 min
t=30 min
Absorbance (au)
Wavelength (nm)
f)
PBS
t=0 min
t=15 min
t=30 min
Absorbance (au)
Wavelength (nm)
g)
DMSO
t=0 min
t=15 min
t=30 min
Absorbance (au)
Wavelength (nm)
h)
PBS
t=0 min
t=15 min
t=30 min
Absorbance (au)
Wavelength (nm)

Supplementary Figure 3. Spectral changes in the UV-vis absorption spectra of (a-b) dynasore, (c-d) dynazo-2, (e-f) dynazo-3 and (g-h) dynazo-4 upon continuous direct excitation with violet light (405 nm, 20 mW, t=minutes) in DMSO (left) or PBS with 1% DMSO (right) respectively.

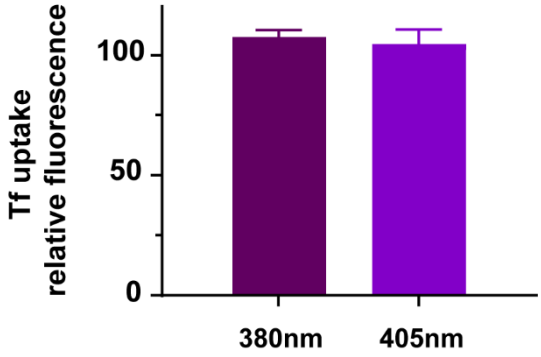

Supplementary Figure 4. Control experiment showing no light effect on Tf uptake in untreated COS7 cells under irradiation at 380 nm and 405 nm relative to Tf uptake in the dark (100% Tf uptake). Data are representative of three independent experiments performed in duplicate and values are expressed in mean ± SEM.

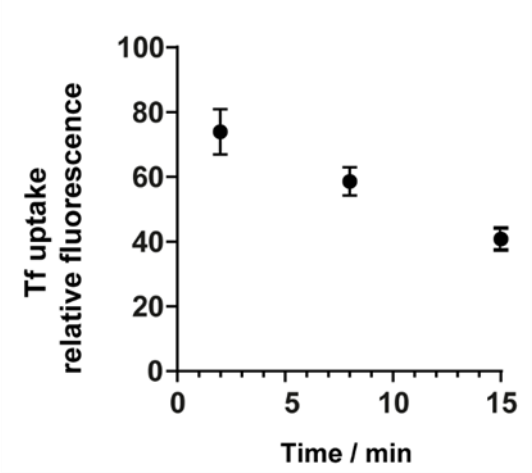

Supplementary Figure 5. Tf uptake time-course in untreated COS7 cells. The internalized labeled Tf was quantified by cytometry for each time point and results are expressed as the percentage of the initial total bound Tf, set as 100%. Data are representative of two independent experiments performed in duplicate and values are expressed in mean ± SEM.

a)

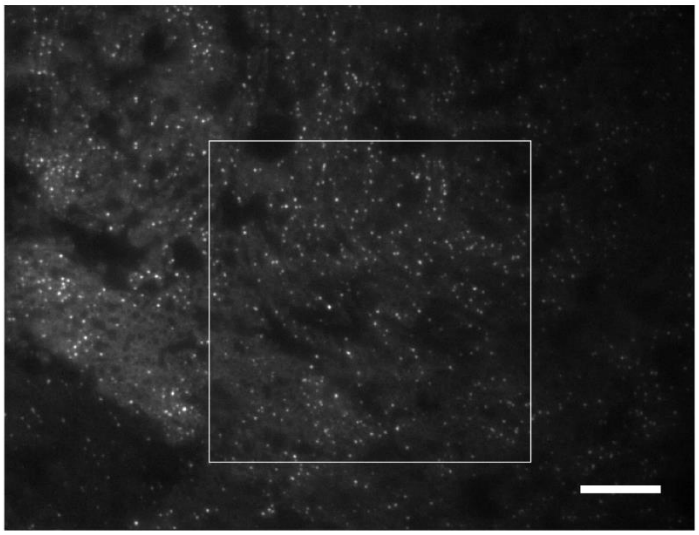

b)

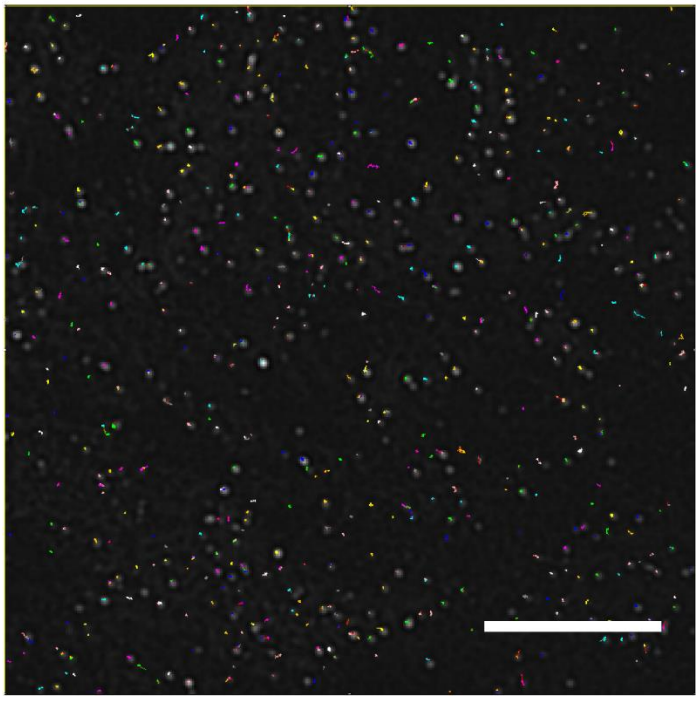

Supplementary Figure 6. A) TIRF microscopy image of a BSC-1 cell footprint displaying fluorescently AP-2-EGFP spots.) B) Trajectories detected in the 40 x 40 µm area shown in the grey box in a) scale bar, 10 µm.

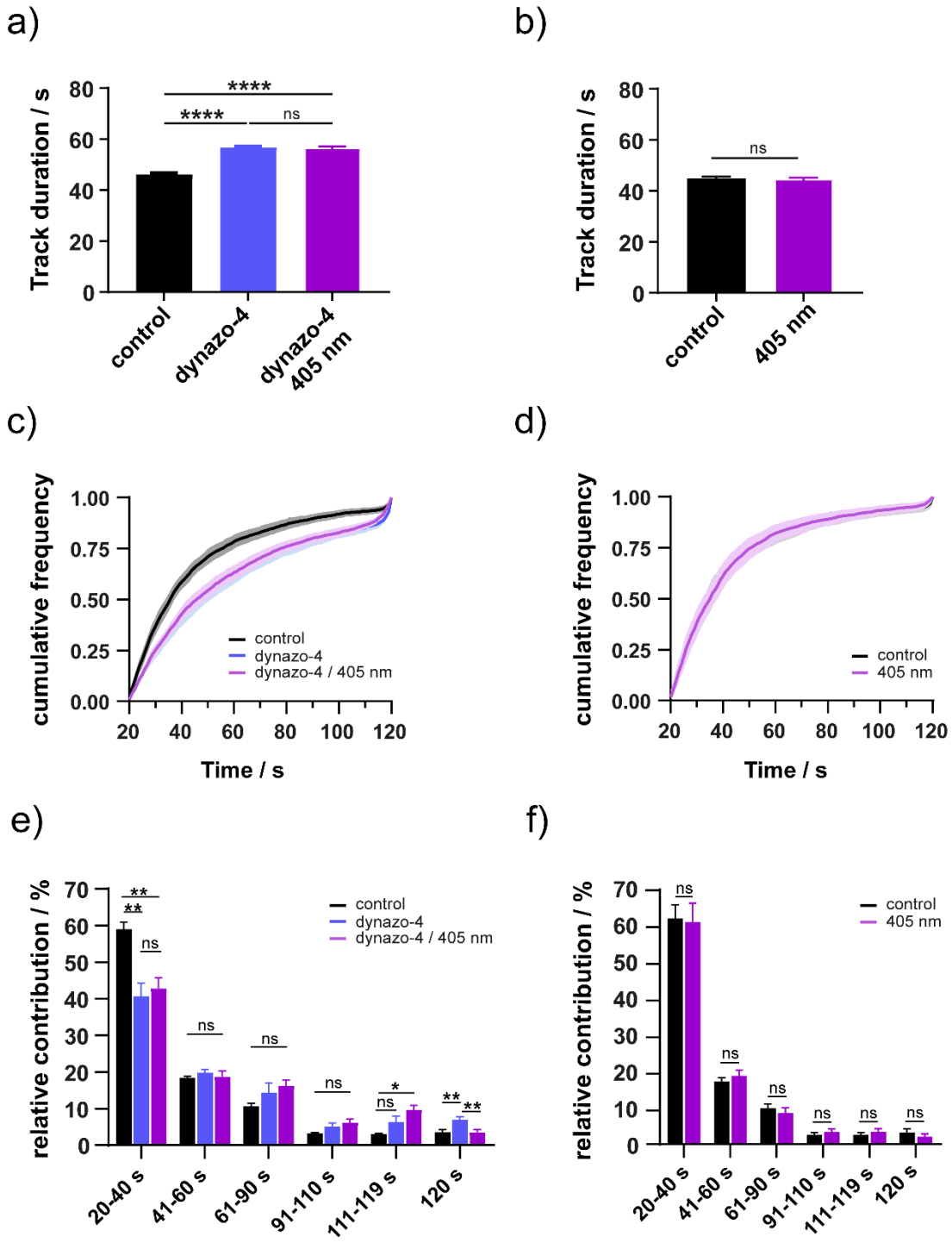

Supplementary Figure 7. Effects of dynazo-**4** and 405 nm illumination on CCP dynamics were analyzed by live-cell TIRF microscopy in BSC-1 cells stably expressing σ2-AP-2-EGFP. A) Mean

CCP duration for control, dynazo-**4** treated cells, and dynazo-**4** treated cells under constant 405 nm illumination. B) Effect of 405 nm illumination on CCP duration in untreated control cells. C) and d) Cumulative plot of CCP lifetime distributions from data depicted in a) and b) respectively. E) and f) Relative contribution (%) of pooled time duration distribution of the detected CCP. The number of trajectories and cells analyzed for each condition in the data depicted in a), c) and e) are: 4510 CCP and n=8 for control cells, 3771 CCP and n=7 for dynazo-4 treated cells and 3154 and n=7 for dynazo-**4** treated cells under constant illumination. The number of trajectories and cells analyzed for each condition in the data depicted in b), d) and f) are: 2414 CCP and n=5 for control cells and 2658 CPP and n=5 for 405 nm illumination. Values are expressed in mean ± SEM. *P < 0.05, **P < 0.01, ****P < 0.0001, ns: non-statistically significant.

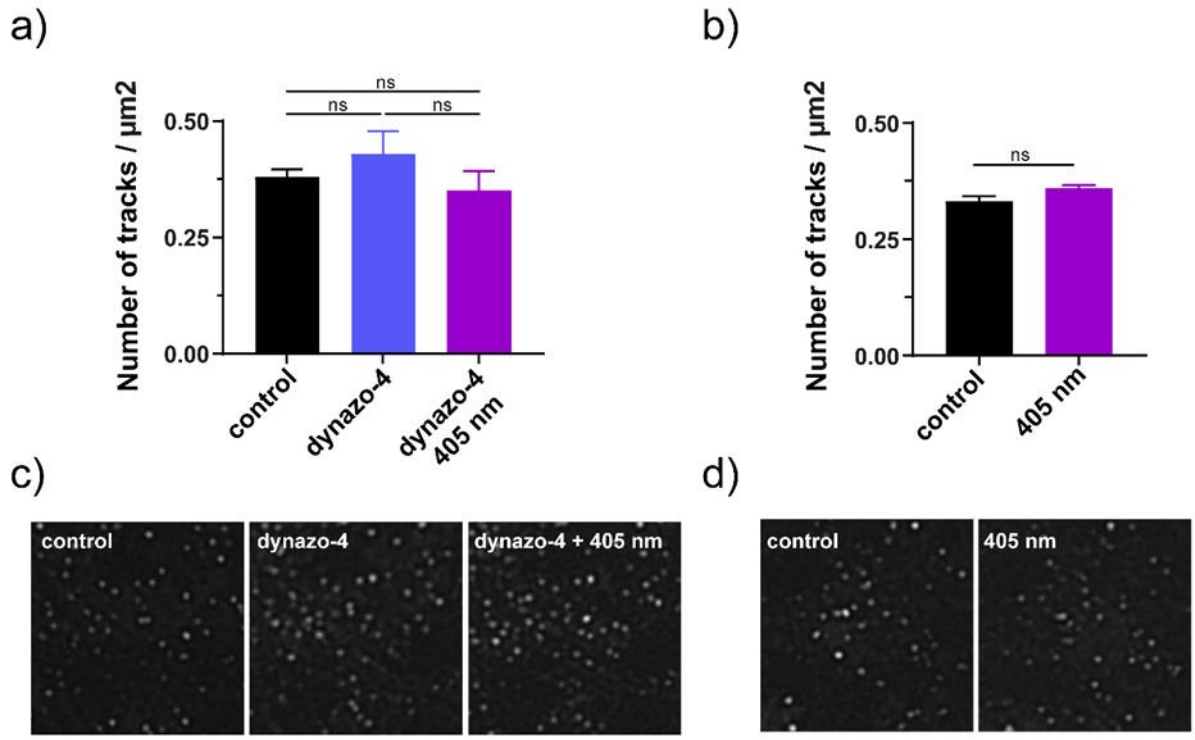

Supplementary Figure 8. A) and b) The number of CPP tracks per square micron on the cell membrane of BSC-1 cells of TIRF experiments shown in Supplementary Figure 7. C) and d) show

representative images of the above results, corresponding to the first frame of the 2 minutes recorded movie for each condition. Ns, non-statistically significant.

Supporting References

1 W. S. Rasband, ImageJ, U.S. National Institutes of Health, Bethesda, Maryland, USA.

2 L. Nevola, A. Martín-Quirós, K. Eckelt, N. Camarero, S. Tosi, A. Llobet, E. Giralt and P. Gorostiza, *Angew. Chemie - Int. Ed.*, 2013, **52**, 7704–7708.

3 I. F. Sbalzarini and P. Koumoutsakos, *J. Struct. Biol.*, , DOI:10.1016/j.jsb.2005.06.002.